STUDY OF STRUCTURAL BEHAVIOR OF THIN FILMS
FIRST YEAR SUMMARY REPORT

By Earl E. Chadsey, Jr., Gabriel E. Padawer,
and Frank Feakes

Prepared Under Contract No. NASW-1553
by
National Research Corporation
70 Memorial Drive
Cambridge, Massachusetts 02142

for

NATIONAL AERONAUTICS AND SPACE ADMINISTRATION

SUMMARY

Earlier work at National Research Corporation had shown that thin films of boron could be made by vacuum evaporating boron onto thin substrates such as aluminum and duPont Kapton, a polyimide film. The layers of boron and substrate could then be bonded together with organic adhesives to form multi-layered structural laminates. These laminates had the important feature that the mechanical properties of the laminate were isotropic in the plane of the laminate.

The present program is an extension of previous work to a more detailed examination of the feasibility of using boron carbide as the reinforcing phase rather than boron.

The chemical composition of the boron carbide varied from 66% to 77% by weight of boron. The composition of the source material was 77% boron as compared to 78.26% boron for stoichiometric formula boron carbide (B_4C).

Some boron carbide films deposited on thick (1/4 inch) substrates and subjected to uniaxial extension fractured only after the normal strain exceeded 5×10^{-3}. Accordingly, the cohesive strength of the film has been calculated as 300,000 psi, or greater. X-ray diffraction studies indicate that the film is "amorphous" with crystallite sizes of less than 50Å.

During the source of the present program, improved procedures were developed for fabricating boron carbide laminates, both with aluminum and polyimide type substrates. An epoxy adhesive (Union Carbide - ERL-2256) was used for the majority of the laminates. Laminates fabricated were subjected to mechanical tests which indicated tensile strengths, elastic modulus, compressive strength, compressive modulus, shear modulus and interlaminar shear strength.

The laminates had the following ranges of properties: 10.9 to 27.3% volume fraction of reinforcement, 4.6 to 16.9 x 10^6 psi tensile modulus, 4.1 to 7.1 x 10^6 psi shear modulus, 13.6 to 28.3 x 10^3 psi tensile strength, 34.0 to 57.4 x 10^3 psi flexural strength, 37.0 to 57.2 x 10^3 psi compressive strength, and 3.7 to 6.7 x 10^3 psi interlaminar shear strength. These values were essentially independent of orientation.

In terms of "specific properties" (i.e., material properties divided by the unit weight of the composite), the maximum results were: specific flexural modulus, 2.63 x 10^8 inch; specific tensile strength, 5.16 x 10^5 inch.

TABLE OF CONTENTS

LIST OF TABLES

LIST OF FIGURES

LIST OF FIGURES

LIST OF FIGURES

LIST OF SYMBOLS

A	crack rate coefficient, $inch^{-1}$
A_o	cross-sectional area, $inch^2$
D	midspan deflection, inch
E_C	compressive modulus of elasticity, $pounds/inch^2$
E_F	flexural modulus of elasticity, $pounds/inch^2$
E_T	tensile modulus of elasticity, $pounds/inch^2$
E_r	Young's modulus of the reinforcement, $pounds/inch^2$
G	shear modulus, $pounds/inch^2$
L	specimen length, inch
M	sample weight, pounds
P	applied load, pounds
T	applied torque, inch-pounds
a,b	linear dimensions, inch
f	crack density, number per inch
ℓ	length of film segment, ($\ell = 1/f$,) inch
t	specimen thickness, inch
w	specimen width, inch
β	post-elastic stress increment, $pounds/inch^2$
ϵ	normal strain, inch/inch
ϵ_{cr}	critical strain, inch/inch
ϵ_f	failure strain, inch/inch
ϵ_{pl}	proportional limit strain, inch/inch
θ	angle of twist, radians
μ	Poisson's ratio, dimensionless
ρ	weight-density, $pounds/inch^3$
σ_C	compressive strength, $pounds/inch^2$
σ_F	flexural strength, $pounds/inch^2$
σ_U	ultimate tensile strength, $pounds/inch^2$
σ_{cr}	critical stress, $pounds/inch^2$
σ_{pl}	proportional limit stress, $pounds/inch^2$
τ	shear traction, $pounds/inch^2$
τ_{max}	interlaminar shear strength, $pounds/inch^2$

STUDY OF STRUCTURAL BEHAVIOR OF THIN FILMS

FIRST YEAR SUMMARY REPORT

Introduction

The general purpose of this investigation was to examine the potential of thin ceramic films as structural materials for space vehicle applications. Previous work at NRC together with programs for the Air Force Materials Laboratory had shown that thin films of boron could be made by evaporation in vacuum onto thin substrates such as aluminum foil and duPont Kapton -- a polyimide film.[1,2] Layers of reinforcement plus substrate could then be bonded together with adhesives to form multilayer laminates which had the important feature that the mechanical properties were isotropic in the plane of the laminate.

While previous work had concentrated on boron films, it had been shown that boron carbide films could be made by similar techniques. The present program was initially directed towards boron carbide and an examination of the possibility of producing silicon carbide films. However, work very early in the program indicated that the potential usefulness of silicon carbide films was considerably lower than that of boron carbide, since silicon carbide does not melt but sublimes at the process temperature and pressure. This, and other technical problems encountered with this material, have been described elsewhere.[3] The present program was therefore confined to the investigation of boron carbide as a reinforcement material.

The main goals of the program were:

(1) Production of adequate amounts of boron carbide film on polyimide and aluminum substrates for subsequent experimental testing work.

(2) Characterization of the principal properties of the films -- particularly chemical composition and general morphology.

(3) Characterization of the mechanical properties of the films -- particularly strength and elastic modulus.

(4) Fabrication of a number of multilayer composites from the films produced.

(5) Development of testing methods applicable to such composite materials followed by testing of a number of composites for the following mechanical properties -- tensile strength, flexural strength, compressive strength, elastic modulus, and interlaminar shear strength.

The results of this program are outlined in the following sections:

2. Material Production

During the performance of this contract specimen materials to be used in obtaining desired data were prepared in two NRC vacuum vapor deposition systems. Most of the materials were prepared in System 421, a semi-continuous facility capable of handling 150 foot lengths of thin metal or plastic sheet. Some of the material was prepared in System 3176, a small batch-type facility capable of coating areas of about 60 square inches. The general procedure used for the evaporation of boron carbide is similar to that used for the evaporation of boron. This has been described by Chadsey and Allen[1] and by Beecher, Feakes and Allen.[2]

The specimen materials were produced by deposition of boron carbide coatings from the vapor phase onto three different substrates. The three substrates were duPont "Kapton"--a polyimide film 0.5 mil thick, aluminum foil 0.7 mil thick, and titanium metal in the form of tapered bars. The titanium substrate specimens were used in a special investigation concerning the intrinsic strength of the vapor deposits, as described in Section 4.

The boron carbide coated 0.5 mil polyimide film was produced in seven runs. Both sides of the substrate were coated. These runs produced approximately 200 feet of 10 inch wide material with a boron carbide coating thickness ranging from 0.12 mil to 0.36 mil. Adhesion of the refractory coating to the polyimide film was characterized by a "Scotch Tape Test" following a two hour exposure of the deposit to boiling water. The adhesion, according to this test, varied from poor to excellent. About 110 feet of material had good to excellent adhesion and was suitable for laminating use.

The boron carbide coated 0.7 mil aluminum foil was produced in four runs in NRC System 421. These runs produced approximately 180 feet of 10 inch wide material with a boron carbide coating, on one side only, ranging in thickness from 0.15 mil to 0.20 mil. The adhesion of the refractory coating to the aluminum foil was excellent. No boron carbide was removed by "Scotch" tape after samples had been immersed in boiling water for two hours.

3. Chemical Composition of Films

A compound such as boron carbide may evaporate in a number of ways. It is possible that the single molecules or associated molecules of boron carbide predominate in the vapor. It is also possible that the boron carbide dissociates with the formation of one or more species such as elemental boron, BC_2, B_2C, etc. Evidence in the literature[4,5] suggests that the main constituents of the vapor are boron, BC_2 and B_2C. Consequently, it is likely that the composition of the condensate formed from the vapor would differ from that of the melt. It is also likely that the deposit formed would not possess the characteristic crystallographic structure of B_4C, even if the atomic ratio were stoichiometric, i.e., 4 to 1.

Although the literature indicates that there are significant differences in the phase rule data on the boron-carbon system, it appears very likely that a solid solution of boron and carbon in boron carbide is possible.[6,7] Consequently, a range of melt compositions is possible around the ideal composition of boron carbide. No data have been found in the literature for the equilibrium liquid and vapor compositions (so-called X-Y diagrams) for the boron-carbon system. In an equilibrium evaporation of a melt having the composition of boron carbide, it is therefore possible that the B-C ratio could change according to whether the boron or carbon had the higher relative volatility.

In the case of electron beam evaporation from the surface of a relatively small crucible of boron carbide, however, the evaporation very likely occurs under non-equilibrium conditions. The liquid phase is mixed by convection currents,

but the degree of mixing from the bottom of the crucible to the evaporating surfaces may not be sufficient to reduce compositional differences to negligible values.

From the foregoing, it is apparent that the true chemical composition of the condensate could not be predicted. We may assume with little error, however, that the average composition of the deposit must agree with that of the feed unless one component was lost by chemical reaction or high vapor pressure.

In the work carried out under the present program a number of analyses were made of the contents of the crucible after an evaporation run. Analyses were also made of the deposit. For all of the evaporation carried out after Run 42-147, the feed material was one composition; 25 pounds of boron carbide from Norton Company was carefully sized, mixed and sampled. Before being used as feed material it was vacuum degassed for 2 hours at 1300°C. Samples of this feed material were analyzed.

The data obtained in the sampling and analytical work are shown in Tables I and II. The theoretical boron content of boron carbide is 78.26 weight per cent boron. The composition of the feed material was 75.3 weight per cent boron.

In general, samples taken from the melt had boron contents slightly higher than those of the feed. The top-center of the melt analyzed about 77 weight per cent in many instances. The data from Run 42-147A1 suggested that the material which climbed up above the melt and froze on the rim of the crucible had a higher boron content than the melt.

The analytical data obtained on the composition of the deposit indicated that it had a lower boron composition than the feed. It was particularly low at the beginning of Run 42-147A1 when the crucible was relatively full with newly melted-in feed.

TABLE I

Composition of Melt

Run 42-145A (End of run)	Top-center of melt	77.13% Boron
	Middle-center of melt	78.19% Boron
Run 42-146A (End of run)	Top-center of melt	77.06% Boron
	Middle-center of melt	76.42% Boron
Run 42-147A1 (Feed composition 75.3% B)	Upper edge of melt	79.6% Boron
	Upper edge of melt	82.3% Boron
Run 42-147A2 (Feed composition 75.3% B)	Top-center of melt	77.46% Boron
	Top-center of melt	76.60% Boron

***

Boron Carbide:	Stoichiometric Composition, B_4C	78.26 wt % B
		21.74 wt % C

TABLE II

Composition of Deposit

Run 42-147A1	Initial deposit Final deposit	67.6% Boron 72.2% Boron
Run 42-147A2	Final deposit	69.5% Boron
Run 3176-28	Total deposit	77.17% Boron
Run 3176-30	Total deposit	77.16% Boron

***

Boron Carbide:	Stoichiometric Composition, B_4C	78.26 wt % B 21.74 wt % C

The data obtained in Run 3176-28 and 3176-30 were from evaporations from smaller crucibles than 42-147A1 and 42-147A2. In the 3176 series, it is likely that the composition would correspond to the removal of relatively large fractions evaporated from the crucible and consequently the analyzed samples would approximate the composition of the crucible feed.

The over-all data suggest that in the evaporation of relatively large volume of boron carbide, initially the carbon has a higher relative volatility than the boron. Under these circumstances the deposits tend to be boron deficient with respect to boron carbide. Over long periods of time, or with large fractions evaporated from the crucible, the composition of the deposits approximates that of the feed.

4. Mechanical Properties of Films

The two mechanical properties of major interest concerning the vapor deposited boron carbide are strength and elastic modulus. Both properties are difficult to measure, mainly because the films are relatively thin and easily damaged. The approach taken in the present work was to use indirect methods for determining both the modulus and the film strength. In the case of the modulus, it has been assumed that void free and well bonded multilayer laminates should obey the Rule-of-Mixtures with respect to the moduli of the composite and components. Since the moduli of both the polyimide substrate and the epoxy adhesives are very low compared to the modulus of boron carbide, the inherent stiffness of the deposited films could be deduced from measurements of the elastic modulus of the composite and the known volume fraction of reinforcement by the Rule-of-Mixtures. Data on this work are presented in Section 7.

The approach used in studying the intrinsic strength of the films is outlined in this section.

Boron carbide was vapor deposited on relatively massive titanium substrate bars. Titanium was chosen because it has a coefficient of thermal expansion ($8 \times 10^{-6}/°C$) which is close to that of boron carbide ($4.5 \times 10^{-6}/°C$). The bars were 1/4 inch thick and tapered in width from 1.0 inch to 0.7 inch over a length of 4.5 inches (Figure 1). The degree of taper was designed to permit the application of a graduated strain amplitude to any thin coating applied to the surface of the tapered bar by means of a single loading.

The tapered bars were polished, cleaned thoroughly and preheated before commencing the coating operation. Coatings of approximately 0.3 mil were applied.

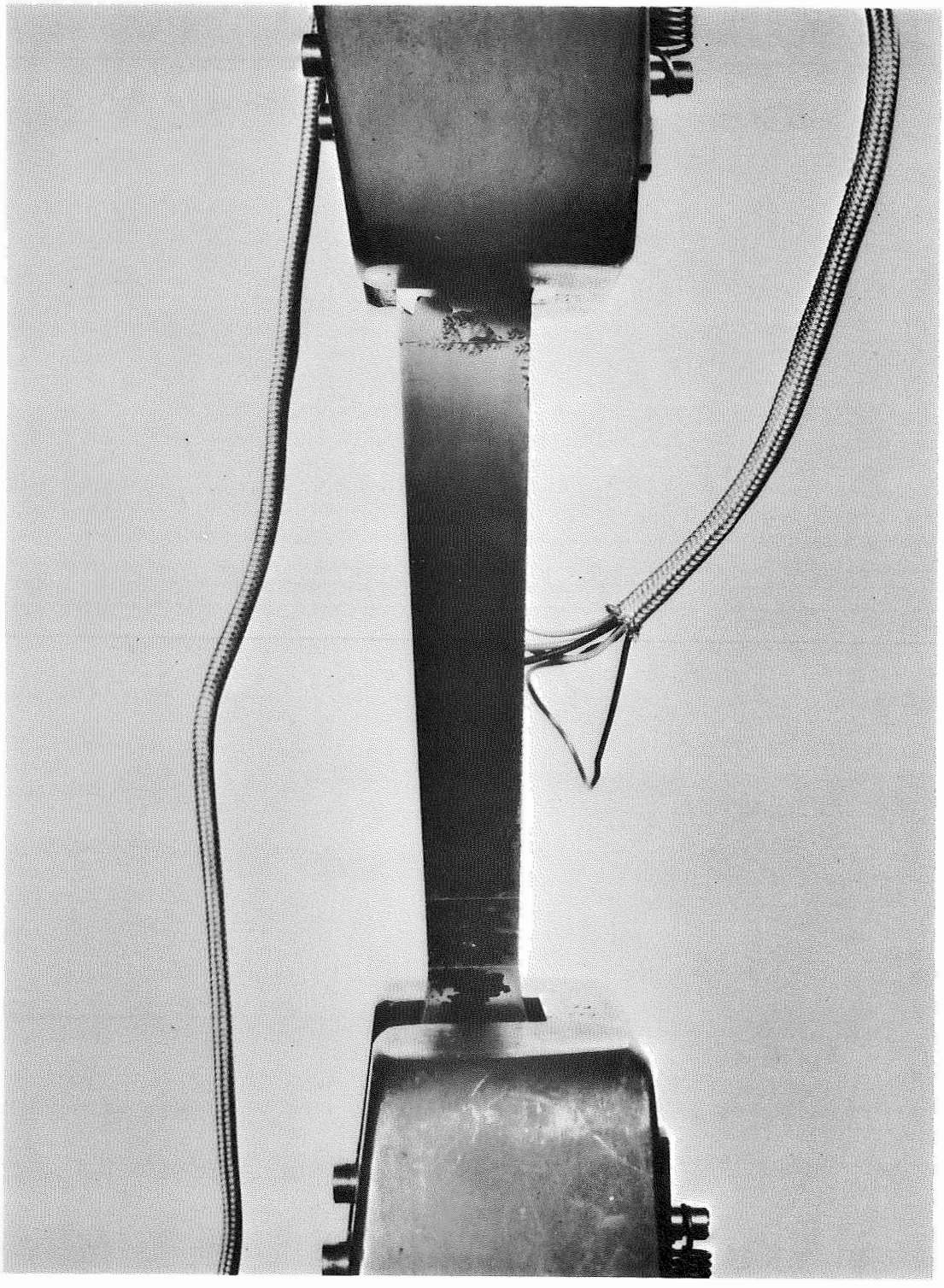

Figure 1

Boron Carbide Coating on
Titanium Taper Bar

The coated bars were pulled in tension in an Instron machine at 0.05 in./min. until a load was reached such that the normal strain in the tapered bar varied from about 0.2% (elastic) at the wider end to about 1.0% (elastic-plastic) at the narrow end. The actual strain distribution was monitored with a series of strain gages (Figure 2). The bar was then unloaded quickly.

The boron carbide film on the front face of the bar behaved like a "brittle coating," such that transverse tension cracks became visible in regions where the cohesive strength of the film was exceeded. With subsequent photographic examination, the density of tension cracks (i.e., number of transverse cracks per unit length of bar) as a function of local strain could be established.

Several coatings were investigated in this way. The coating runs and some of the associated coating parameters are shown in Table III.

The results have been represented by a plot of linear crack density, f, vs. maximum local strain ϵ, as shown in Figure 3.

The data indicated that boron carbide films could be characterized by a rather sharp critical failure strain, ϵ_{cr}, at which the first tension cracks occurred. (The "critical strain", ϵ_{cr}, was determined by extrapolating the observed data to $f = 0$, i.e., no cracks.) Additional cracks appeared very rapidly with a small increase of the strain, such that for all practical purposes the material had failed when ϵ_{cr} was exceeded. (In this respect, these boron carbide films resembled the conventional engineering materials more than the glassy ceramics for which the strength distribution usually covers a much broader spectrum.)

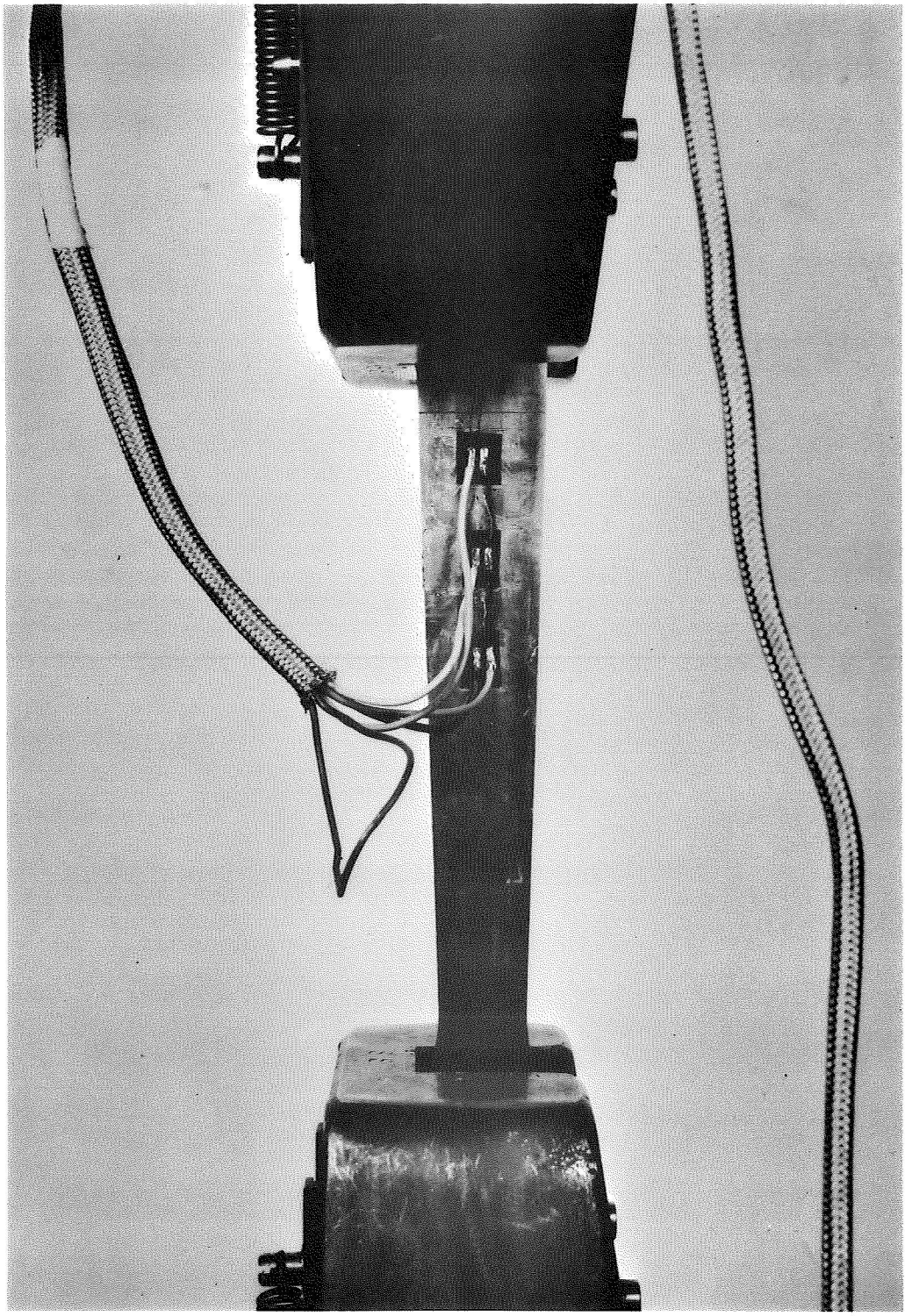

Figure 2

Monitoring the Elastic-Plastic Strain
Distribution in Titanium Taper Bars

TABLE III

Boron Carbide Film Coated
on Titanium Taper Bars

Bar No.	Date Coated	Coating System (a)	Substrate Temperature °C (b)	Remarks
Ti 1	4-67	421	600	Poor adhesion, excessive debonding
Ti 2	4-67	421	600	Good adhesion, many globular irregularities embedded in coating surface
Ti 23	10-67	3176	530	Good adhesion, smooth surface
Ti 24	11-67	421	625	1. Smooth polish on substrate 2. Substrate textured with 2/0 grit abrasive in transverse direction
Ti 25	11-67	421	625	1. Smooth polish on substrate 2. Substrate textured with 2/0 grit abrasive in longitudinal direction
Ti 26	1-68	3176	220	Poor adhesion, excessive debonding
Ti 27	1-68	3176	600	1. Edges of deposit diffuse by masking 2. Edges cut sharp with diamond wheel

(a) Coating system: 421 = larger (~40 cu. ft.) vacuum chamber.
3176 = smaller (~6 cu. ft.) experimental coater.

(b) Substrate temperature: as indicated by thermocouple placed in vacuum behind substrate bar. Gave only approximate reading of true surface temperature.

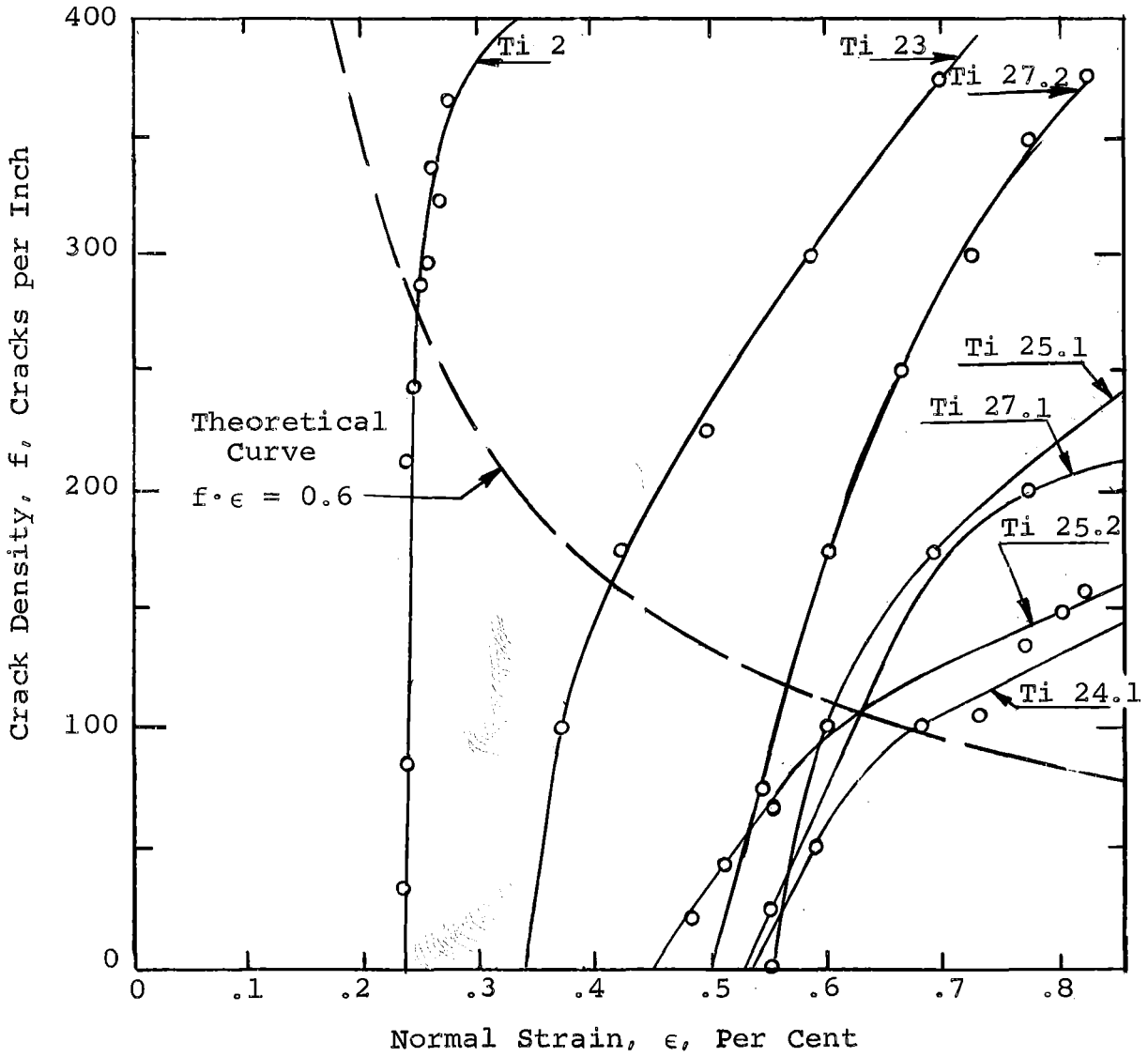

Figure 3

Crack Density Distribution in
Boron Carbide Thin Film Coatings

Values for ϵ_{cr} for the several types of specimens ranged from a low 0.23% to a high 0.55%. Assuming perfectly brittle-elastic behavior and a Young's modulus of 60×10^6 psi for boron carbide, the corresponding fracture strengths ranged from 138,000 to 330,000 psi.

The observed behavior could be described analytically by the function

$$f(\epsilon) = 0, \quad \epsilon < \epsilon_{cr} \qquad (1)$$
$$= A(\epsilon - \epsilon_{cr}), \quad \epsilon > \epsilon_{cr}$$

where $f(\epsilon)$ = the strain dependent crack density (in^{-1})

ϵ = the local value of the normal strain (in/in)

A = a numerical coefficient, (in^{-1})

ϵ_{cr} = value of the "critical strain" (in/in)

Numerical values for ϵ_{cr} and A are shown in Table IV.

The linear crack rate coefficient, A, approximates the observed behavior quite well, up to a certain limit, indicated in Figure 3 by the theoretical curve $f \cdot \epsilon$ = constant. This function is derived, and the constant is evaluated, in Appendix I. There it is shown that a much smaller rate of crack accumulation must be expected beyond this limit, because the ultimate shear strength of the titanium substrate has been reached. Below this limit, however, the rate of formation of tension cracks in the boron carbide film is not affected by the strength limitations of the substrate material.

The observed variation of ϵ_{cr} from specimen to specimen could be correlated in some cases with the coating parameters indicated in Table III as follows:

TABLE IV

Critical Fracture Strains and
Crack Rate Coefficients for Boron Carbide Films
on Massive Substrates

Bar No.	ϵ_{cr} % (a)	A $in.^{-1}$ (b)
Ti 2	.23	30×10^6
Ti 23	.34	3.3×10^5
Ti 24.1	.54	1.2×10^5
.2	.50	(c)
Ti 25.1	.55	2.3×10^5
.2	.45	0.7×10^5
Ti 27.1	.53	1.1×10^5
.2	.50	1.8×10^5

(a) Critical strain, $f = 0$ for $\epsilon < \epsilon_{cr}$.

(b) Crack rate coefficient defined by Eq. (1). Valid for the range

$$\epsilon_{cr} < \epsilon < \frac{0.6}{f} .$$

(c) Transverse surface roughness made crack counting very difficult. Only the first crack in the critical strain region was located.

(1) Fabricating experience: coatings produced in the latter half of the program exhibited improved strength.

(2) Deposition temperature: at indicated substrate temperatures less than about 600-625°C, the coating-to-substrate bond was weak and the strength of the film was low. Above this temperature, the critical strain was fairly uniform at 0.5% ±.05%, from which an inherent tensile strength of, say, 300,000 psi could be deduded.

(3) Coating system: material produced in the larger (421) or smaller (3176) coating system could not be distinguished in these experiments.

(4) Substrate surface preparation: two substrate bars were polished smooth (experiment parts 24.1, 25.1), but then were striated with 2/0 grit abrasive parallel (part 25.2) or transverse (part 24.2) to the bar axis for one-half their length prior to coating. Repeated testing indicated that the roughened substrate surface increased the crack frequency only slightly. A reasonable explanation for this would be that even a "smoothly" polished surface contains sufficient microscopic irregularities to affect the coating like a "rough" surface.

(5) Coating edge preparation: film coating on one bar (Ti-27) was left with the diffuse shadowed edge produced by masking for half the bar length (part 27.1); for the remainder, the lateral edges were trimmed sharp by means of a diamond grit slitting wheel (part 27.2). Repeated testing indicated that a slightly higher crack rate and a lower critical strain were associated with the edge trimming operation. Apparently, the use of a cutting wheel introduced additional edge damage which, when stressed in tension, intensified the cracking. The fractional increase was small, however, suggesting that a large number of crack sources was already present in the diffuse edge or in the surface of the coating.

The optical examination of the cracks showed them to be nearly straight and continuous, edge to edge. Crack origins were not easily identifiable with optical microscopy. Both carbon and parlodion replicas were studied with electron microscopy at higher magnification, but the replication techniques were very difficult and it is not certain that all of the features observed were due to the original boron carbide surface. The topography of fine cracks, in particular, tended to be obscured since the replica material could not be separated neatly. Some useful photographs were obtained, however, and are shown in the next section.

Summary of Results

(1) The boron carbide vapor deposited films, under certain conditions, exhibited breaking strengths on the order of 300,000 psi.

(2) The breaking strength of boron carbide film was a relatively sharp function of the imposed strain. A critical strain, ϵ_{cr}, was identified.

(3) The breaking strength of boron carbide was strongly dependent on substrate deposition temperature, but only a weak function of substrate surface texture or edge treatment (within the observed range of these variables).

5. Morphology Studies

Mounting and replicating techniques have been developed to permit the microscopic examination of virgin and fractured specimens. Both electron and optical microscopy were employed.

Electron Microscopy

Fresh boron carbide film surfaces, and also transverse fracture surfaces, have been examined by means of replication techniques, with varying degrees of success. Replicas were made with 1% parlodion solution, 3% parlodion solution, or by the 2-stage acetate tape/carbon vapor process. Carbon balls were dusted onto the replica surface in some instances to introduce known shadow lengths and directions for comparison. Chromium vapor at 50° incidence was used for shadowing all replicas.

Selected electron micrographs are shown in Figures 4-8 and may be described as follows:

- Figure 4: Surface of Ti-23 bar coating. The surface was relatively smooth and even, except for occasional fissured flaws. These may be effective nuclei for tension cracks when stressed, but the observed area density of this particular kind of flaw was much smaller than the density of cracks which appeared after testing. Other types of flaws or discontinuities therefore must be equally effective stress raisers.

- Figure 5: Surface of Ti-23 bar coating. Some isolated areas appeared rough and uneven. These were ascribed to "spits", i.e., areas where liquid droplets of the melt reached the substrate.

- Figure 6: Surface of Ti-24 (polished substrate) bar coating. The coating surface here was somewhat uneven,

Figure 4

Electron Micrograph of the
Surface of Ti-23 Bar Coating, 11000X

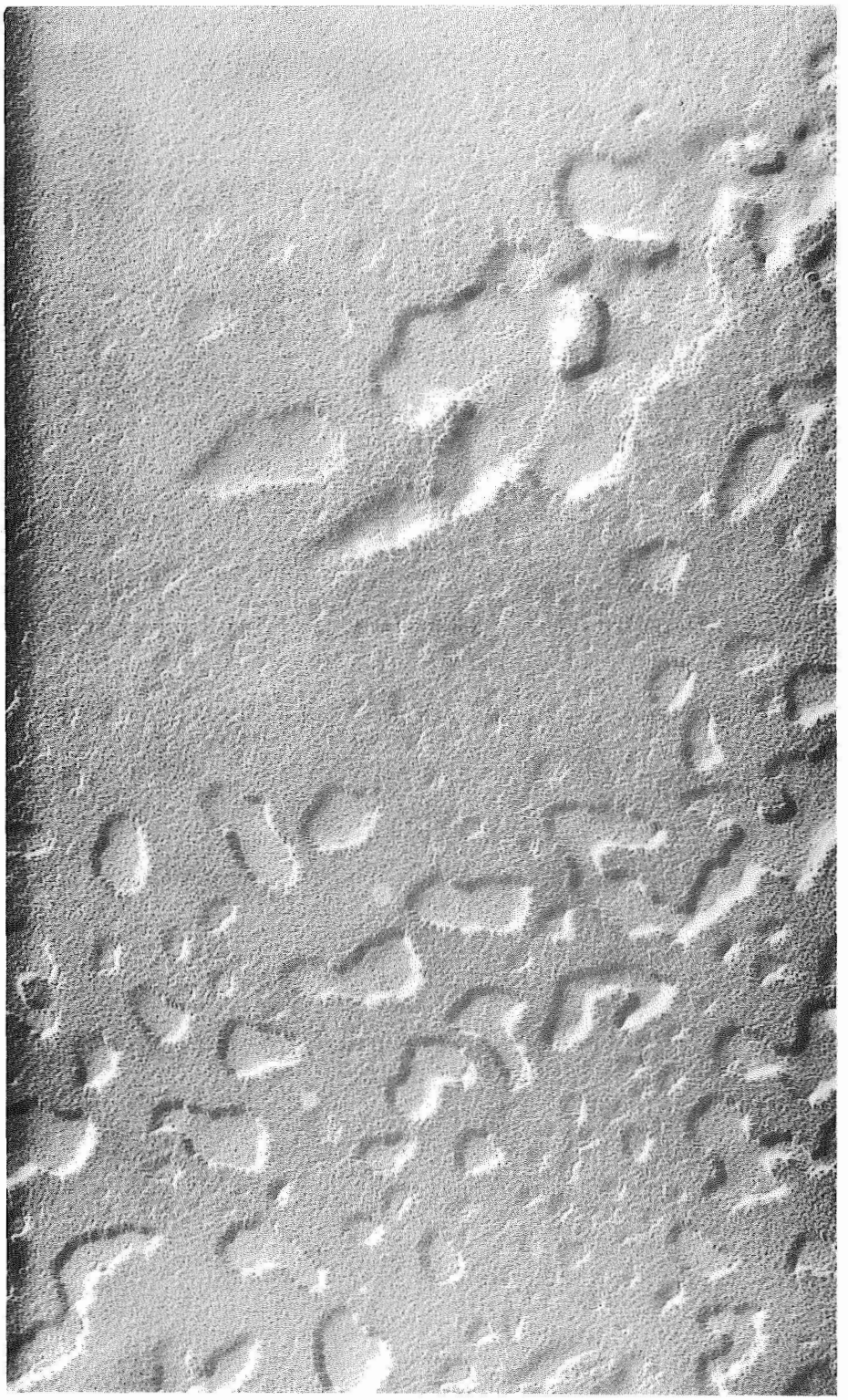

Figure 5

Electron Micrograph of the Surface
of Ti-23 Bar Coating, 55700X

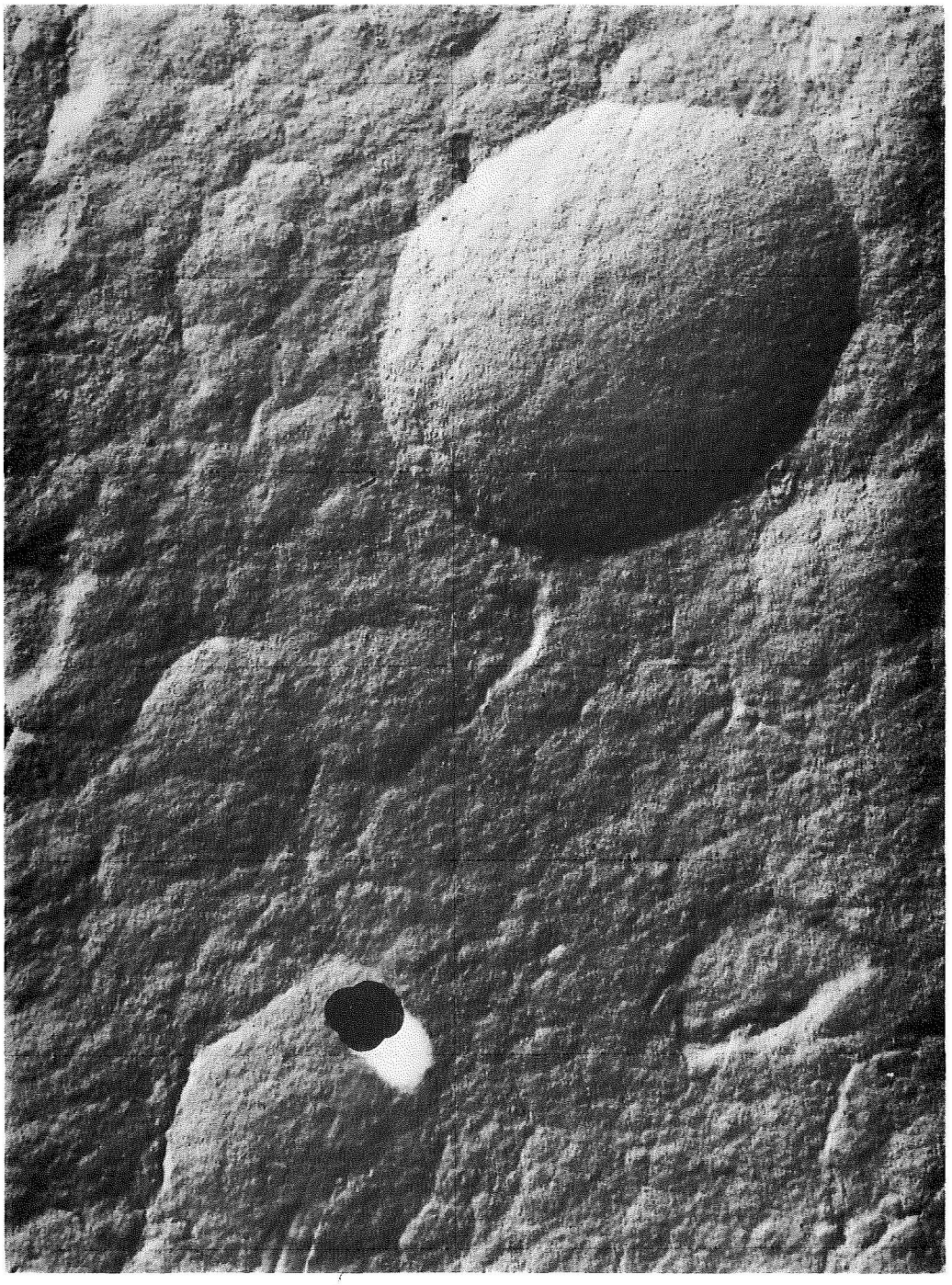

Figure 6

Electron Micrograph of the Surface of Ti-24
(polished substrate) Bar Coating
(Carbon Balls Indicate Shadow Direction, 11580X)

and included many "domed" or "mounded" protuberances. These could possibly be due to preferential precipitation of the vapor in the neighborhood of some growth-promoting nuclei.

- Figure 7: Surface of Ti-25 (polished substrate) bar coating. A similar "mounded" structure was observed here. The "valley floor" surrounding the "mounds" was relatively smooth and even textured.

- Figure 8: Surface of Ti-25 (rough, striated substrate) bar coating. The striations of the substrate have been reproduced quite prominently by the coating. Otherwise, the coating surface texture resembled that of the smooth substrate sample (Figure 7). Some holes or depressions, probably due to "spitting" appear to have collected in the troughs of the striated surface.

Replicas of boron carbide film cross-sections were much more difficult to produce, because the jagged fracture edges which were characteristic of transverse sections of this very hard and brittle material caused tearing of the replica upon separation. More recently, improved replicating methods have been developed, but no micrographs of sufficient quality are available for this report.

Photo-micrographs

A number of surface and section photographs of boron carbide laminates have been made. Since most of these show the failure region of tested specimens, they are shown in the next section together with the description of the method of test and the results.

X-ray Diffraction Studies

During the cource of the present program samples of boron carbide deposits were taken for X-ray diffraction studies. In general, the patterns produced by the deposits were diffuse

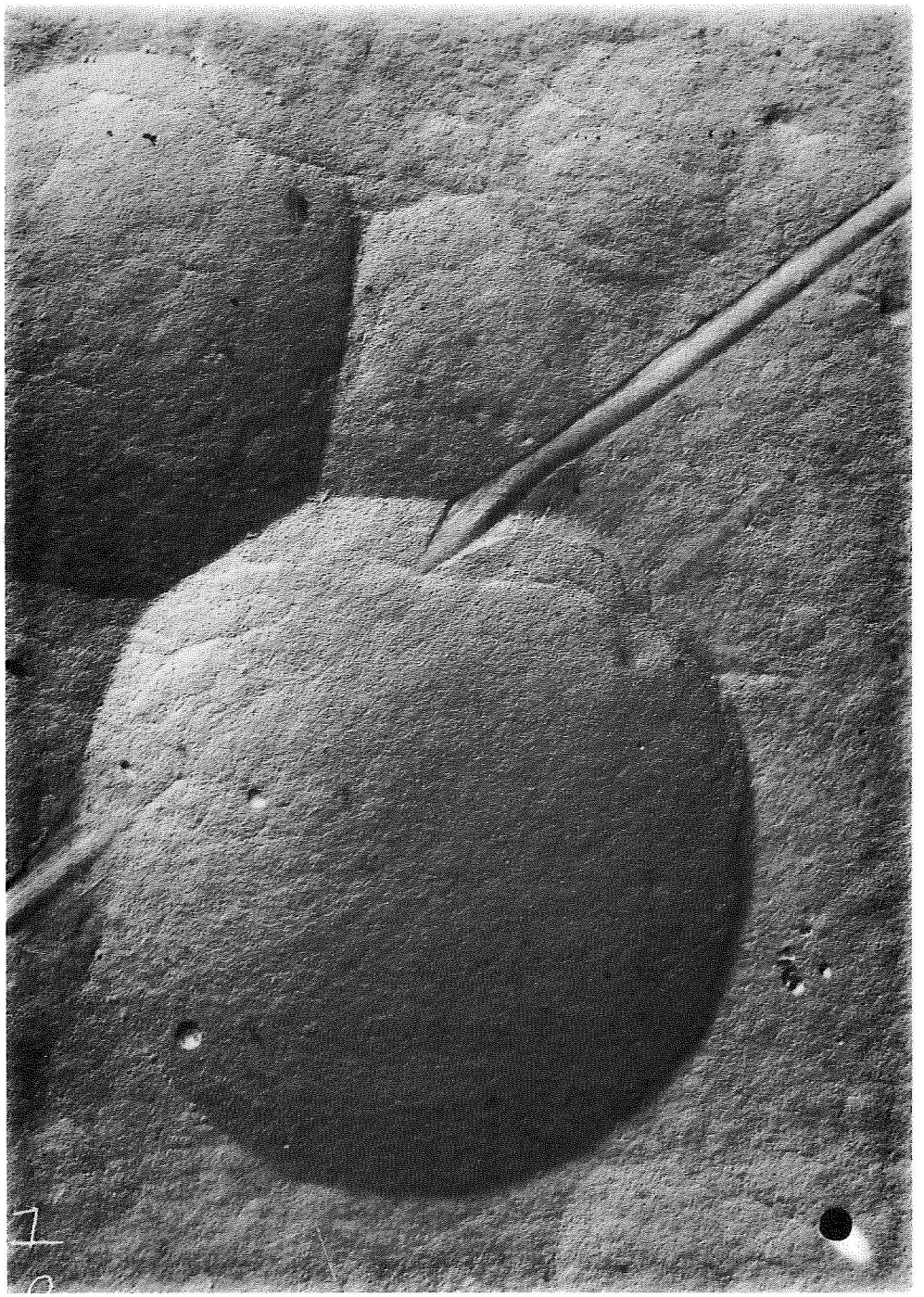

Figure 7

Electron Micrograph of the Surface of
Ti-25 (polished substrate) Bar Coating
(Carbon Balls Indicate Shadow Direction, 11580X)

Figure 8

Electron Micrograph of the Surface
of Ti-25 (striated substrate) Bar Coating
(Carbon Balls Indicate Shadow Direction, 11580X)

and indicated that the deposits were typically "amorphous" in character. A typical X-ray diffraction photograph is shown in Figure 9. The exposure conditions used were Copper $K\alpha$ radiation, 35 KV, with an exposure time of 3 hours. In selecting the samples for examination, several variables were considered. For instance, three samples were taken to estimate whether there was any variation in the crystallite size as a function of the thickness of the deposit. In Table V, Sample No. 695B was a thin deposit (approximately 0.1 mil), 696A - a deposit of medium thickness (approximately 0.2 mil), and 692A - a thick deposit (approximately 0.3 mil). All of these deposits were removed from 0.5 mil polyimide film and the temperature of the coating plate adjacent to the substrate during deposit was relatively low, 150-170°C. In comparison, sample 690A was deposited on titanium foil held at 530°C during deposition. The deposit thickness was relatively thin (approximately 0.1 mil).

A sample was also taken of the boron carbide material from the crucible. This material had been vacuum degassed by electron beam melting, but had resolidified within the crucible. It was the normal evaporation source material.

From the degree of line broadening in the X-ray diffraction photographs, estimates were made of the average crystallite size. The results are presented in Table V.

In general, the data indicate that there is no significant variation in crystallite size with deposit thickness, or with the substrate temperature during deposition. The estimated values of the crystallite sizes are sufficiently low that it is unlikely that the strengths of the films would be determined by the inter-crystal strength (grain boundary) as in more highly crystalline materials.

TABLE V

Boron Carbide, X-ray Data

Sample No.	Run No.	Estimated Crystallite Size	Deposit Parameters
695B	42-146B	23Å	Poly. Sub. 170°C, Thin
696A	42-149B2	46Å	Poly. Sub. 165°C, Medium
692A	42-138B	37Å	Poly. Sub. 165°C, Thick
690A	3176-B	46Å	Ti Sub. 530°C, Thin
703B		~2000Å	Source Material

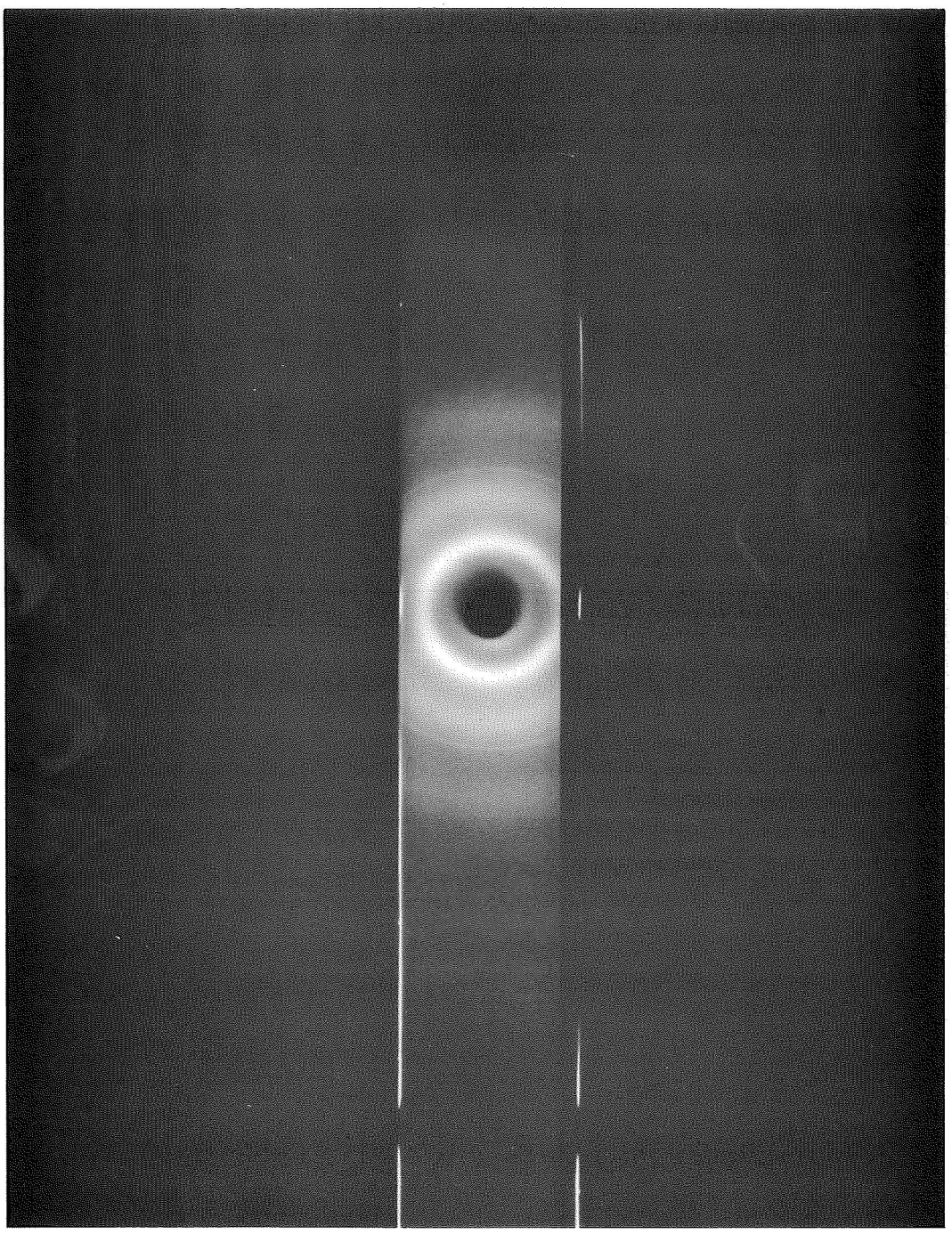

Figure 9

X-Ray Photograph of Boron Carbide Flake,
Sample No. 692A
(Cu K Radiation, 35 kv, 3 Hours Exposure)

6. Fabrication of Composites

Previous work at NRC,[1,2] had shown that multilayered laminates could be made from the sheets of reinforcement on substrate with a large variety of adhesives such as epoxy (Shell Epon 828 and Shell Epon 815), phenoxy (Union Carbide PKSB-8085), and a variety of polyimides. Of these, the phenoxy PKSB-8085 initially appeared to have a satisfactory combination of properties. Important among these were a simple curing procedure and the ability to control the glue line thickness. Prior to the present contract a number of composites were made with the phenoxy material. However, poor results were obtained occasionally. Bubbles appeared in the laminate after removal from the press. At first it was thought that these bubbles resulted from either entrapped air or solvent released during curing at 190°C. The use of vacuum to remove air and solvent did not greatly improve the laminates. During the early work on the present program, a series of laminating tests with transparent Kapton film showed that many of the bubbles were, in fact, voids with little, if any, gas content. The bubbles appeared to be caused by poor adhesion of the phenoxy to the reinforcement. Poor wetting along with the low viscosity of the phenoxy resulted in poorly bonded regions in the laminate. Consequently, when the laminate cooled after curing, the polyimide contracted more than the reinforcement and a "bubble" formed.

During the initial work on the present program, three laminates were made with PKSB-8085. Two of these (2848-12 and 2848-16) had so many bubbles that testing work was not warranted. On the other hand, laminate No. 2848-14 had relatively few bubbles and test data presented later within this report were obtained for it.

On the advice of Mr. James Ray of the Air Force Materials Laboratory, a number of preliminary laminating tests were completed with Union Carbide Epoxy ERL-2256. This adhesive has been well characterized by previous workers and is known to have good wetting properties for boron filament. The preliminary tests showed considerable promise. A transparent laminate made with Kapton film and ERL-2256 had very few bubbles, good adhesion and a reasonable glue line. Following this, four boron carbide - Kapton laminates were made with ERL-2256 to develop a laminating procedure and to prepare samples for comparison of PKSB and ERL-2256 as adhesives in this type of laminate. Table VI lists the composition of all laminates made on this program.

The ERL-2256 comparison laminates are Nos. 2844-17, 2848-20, 2848-26, and 2848-28. Development of a laminating procedure for these laminates demonstrated the following advantages for this adhesive over PKSB-8085:

(1) ERL-2256 wets boron carbide more readily.

(2) ERL-2256 requires lower laminating pressures.

(3) ERL-2256 cures at a lower temperature (180°F vs. 300°F).

While the boron carbide films used in the ERL-2256 comparison laminates were thin and of variable quality, the laminates demonstrated that definite advantages resulted from the use of ERL-2256 and work with PKSB was discontinued.

The following standard procedure was used for the early laminating work using ERL-2256 as the adhesive:

(1) Material to be laminated was sampled, weighed, and cut to size.

(2) Sheets were then cleaned by dipping in warm acetone followed by hot ethanol.

TABLE VI

Laminate Composition

Cure Date	Laminate No.	No. of Layers	Vol % Rein.	Remarks
3/28/67	2848-12*	20	15.4	Bubbles not tested
3/31/67	2848-14*	20	18.9	Few bubbled - tested
4/6/67	2848-16*	20	11.8	Bubbles - not tested
4/7/67	2844-17	20	18.6	Evaluation of ERL-2256
4/12/67	2848-20	20	16.3	Evaluation of ERL-2256
4/15/67	2848-26	20	14.5	Evaluation of ERL-2256
4/25/67	2848-28	20	18.1	Evaluation of ERL-2256
6/14/67	2848-28E	80	15.8	Secondary: Comp. Test
6/14/67	2848-28F	80	16.2	Secondary: Comp. Test
6/14/67	2848-28G	80	15.5	Secondary: Comp. Test
6/22/67	2848-14E	80	16.3	Secondary: Comp. Test
6/28/67	2848-28H	80	15.9	Secondary: Int. Shear Test
6/29/67	2848-28I	80	17.0	Secondary: Int. Shear Test
10/25/67	40-42	20	27.3	Standard Laminate
10/31/67	40-49A	2	29.7	Glue Line Study
10/31/67	40-49B	2	30.4	Glue Line Study
10/31/67	40-50A	2	30.7	Glue Line Study
10/31/67	40-50B	2	29.9	Glue Line Study
11/2/67	40-47	20	23.9	Standard Laminate
11/8/67	40-55	8	30.4	Secondary: Made from 40-49 A&B; 40-50 A&B
11/16/67	40-42C	80	24.9	Secondary: Int. Shear Test
11/16/67	40-47C	80	23.5	Secondary: Int. Shear Test
11/22/67	40-69**	20	16.8	Standard Laminate
11/22/67	40-42E	80	26.4	Secondary: Comp. Test
11/22/67	40-47E	80	23.7	Secondary: Comp. Test
11/29/67	40-72	20	17.5	Standard Laminate
1/12/68	40-69E**	120	16.5	Secondary: Int. Shear Test
1/12/68	40-69F	120	16.2	Secondary: Int. Shear Test
1/12/68	40-72E	120	17.3	Secondary: Int. Shear Test
1/12/68	40-72F	120	16.8	Secondary: Int. Shear Test
1/26/68	40-88	20	15.3	Standard Laminate

*PKSB was used for these laminates. An epoxy adhesive, ERL-2256 was used for other laminates listed.

**Boron carbide - aluminum was used for these laminates.

(3) When dry (a few minutes in air) the sheets were dipped in the adhesive mixture ERL-2256 (100 parts by weight) to curing agent Z (20 parts by weight) diluted with an equal volume of methyl ethyl ketone.

(4) The sheets were hung in the air oven at 90°C until tacky -- approximately 20 minutes.

(5) The sheets were laid up with a layer of undiluted adhesive mixture between each layer in the bottom chamber of the vacuum press. See Figures 10 and 11.

(6) The laminate package was then evacuated to less than 200 microns without applying any pressure to the laminate. This was done by evacuating both the top and bottom chambers after assembling the press. Figure 12.

(7) Pressure was slowly applied to the package first by admitting gas to the upper chamber, and then exerting pressure (200 psi) on the laminate through the diaphragm. The mechanical press was used for this operation.

(8) Heat was applied to cure (1 hour at 180°F) followed by a post cure of 1 hour at 300°F.

The standard laminate consisted of 20 layers of reinforcement material held together by 19 layers of adhesive. This package, which had an average thickness of 20 mils, was considered to be too thin for practical compression and short beam interlaminar shear tests. Laminates for these tests were prepared by cutting a standard laminate into smaller specimens (see Section VI) and relaminating these to produce a secondary laminate with a smaller area but having four to six times the thickness of the original. The 80 and 120 layer laminates listed in Table VI were prepared in this manner.

The standard laminating procedure previously described was modified as a result of the glue line study involving

VACUUM PRESS ASSEMBLY

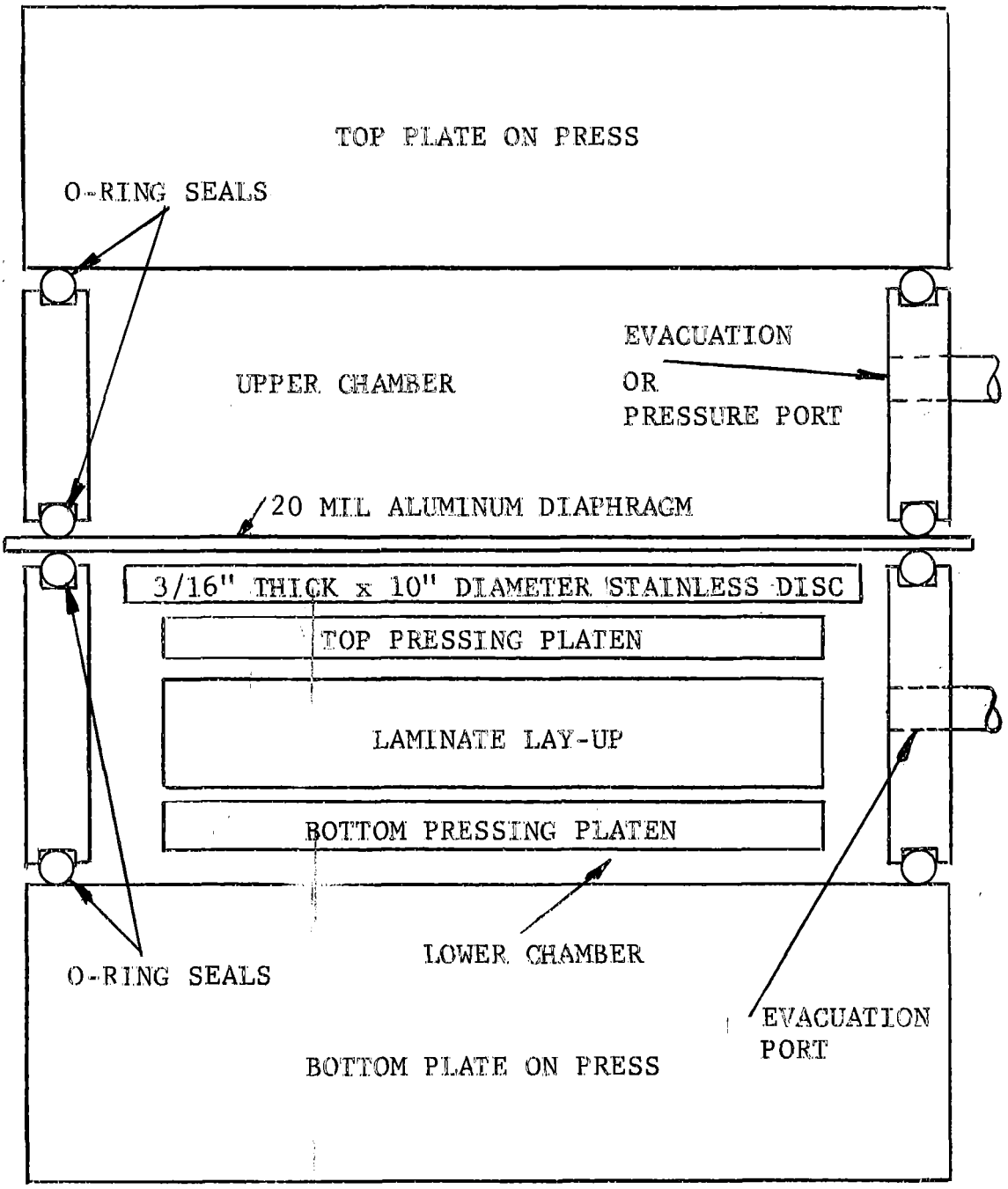

Figure 10

Vacuum Press Assembly for Fabricating Boron Carbide Sheet Reinforced Laminates. (Schematic)

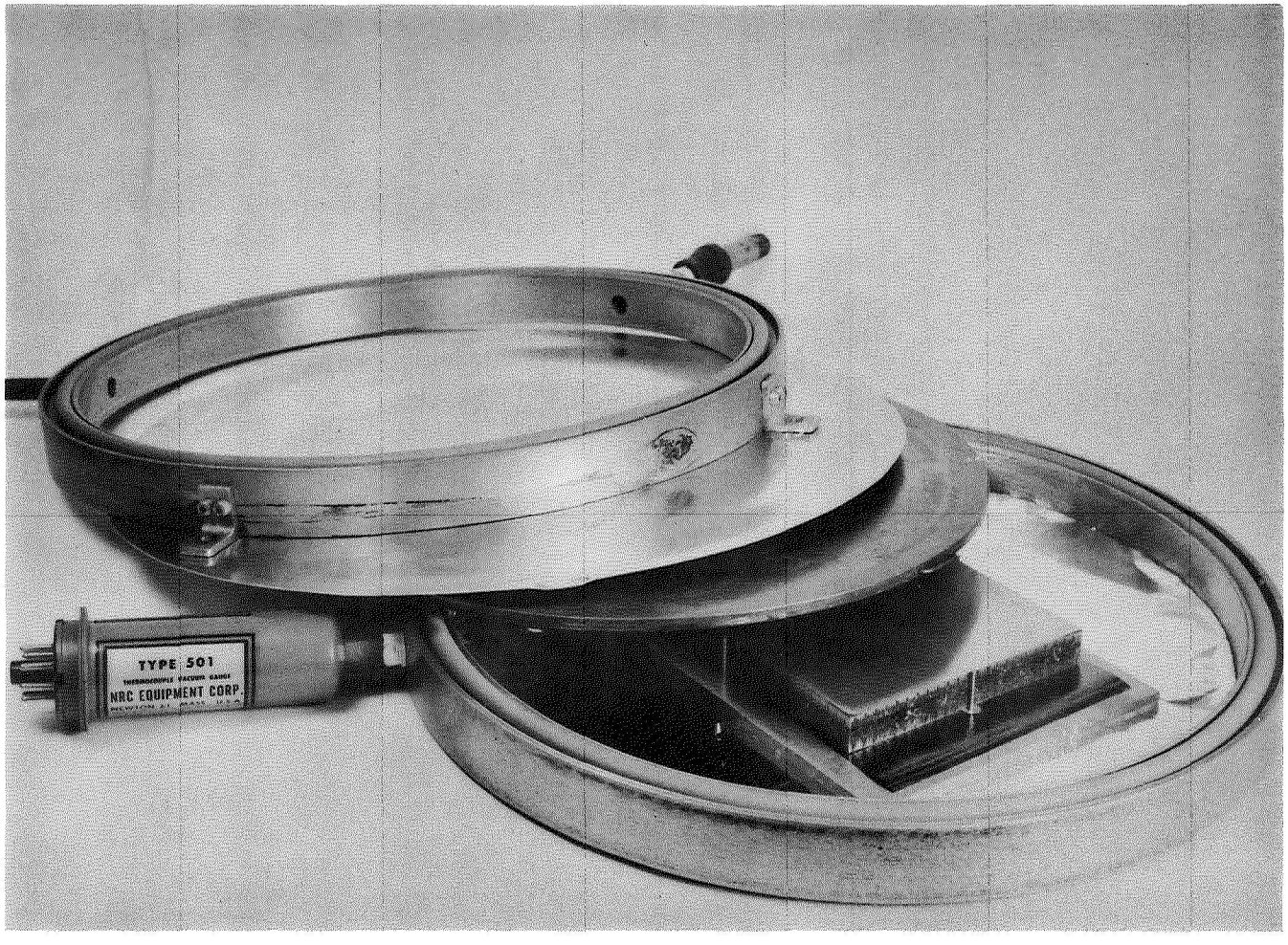

Figure 11

Lay-up of Laminate in Vacuum Press

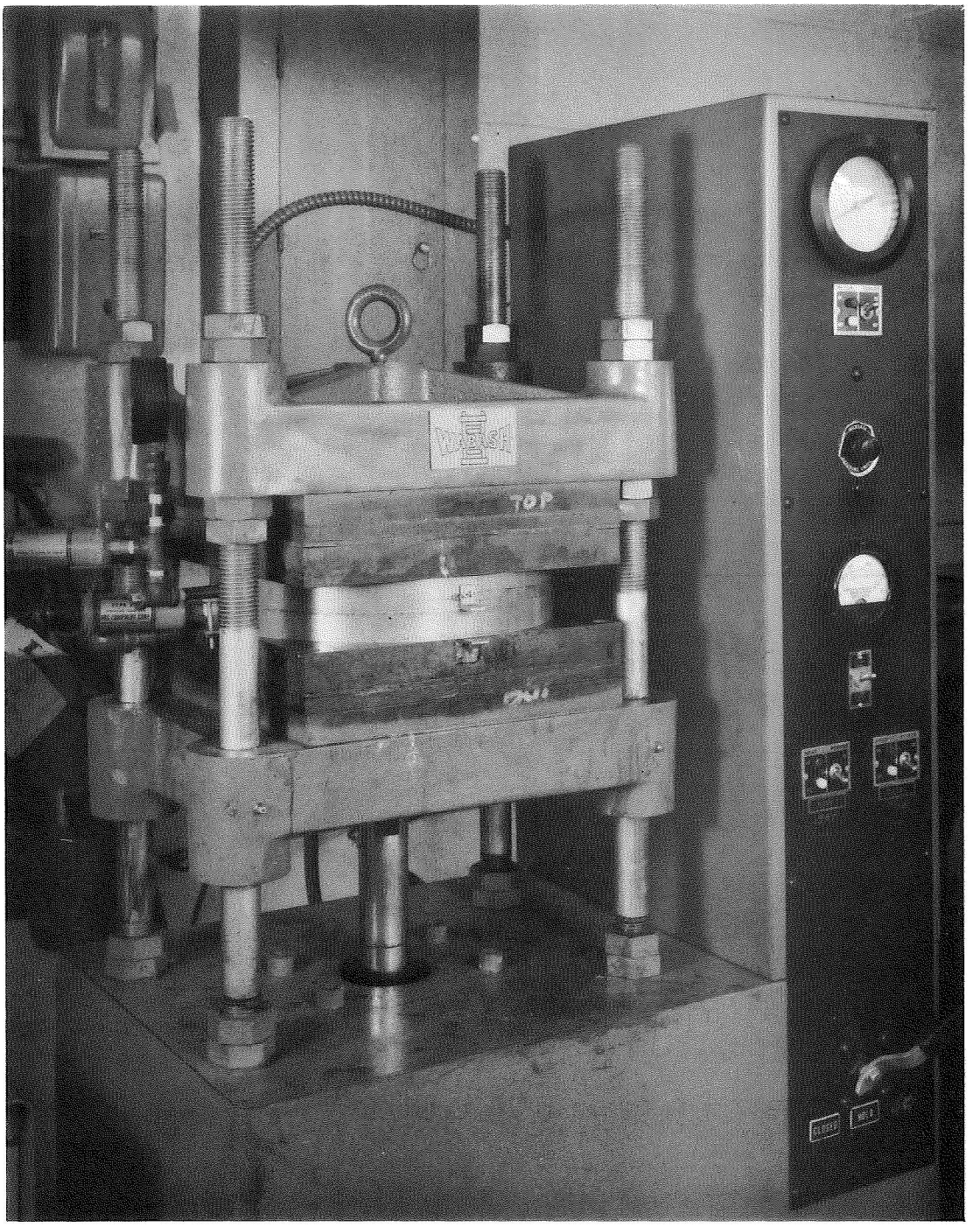

Figure 12

Vacuum Press Assembled in Mechanical Press

laminates 40-49, 40-50, and 40-55. The resultant final standard laminating procedure is outlined below:

(1) Material to be laminated is sampled, weighed, cut to size, and measured.

(2) Sheets are then cleaned by thorough spray rinsing with warm acetone followed by hot alcohol.

(3) When dry (a few minutes in air), the sheets are wet spray coated with an adhesive mixture of ERL-2256 (100 parts by weight) and curing agent Z (20 parts by weight) diluted with 9 times its volume of methyl ethyl ketone.

(4) The sheets are then drained in air 5 minutes and hung in an air oven at 225°F for 45 minutes.

(5) The precoated sheets are then wet spray coated with the same adhesive mixture diluted with an equal volume of methyl ethyl ketone.

(6) The sheets are then drained in air 5 minutes and hung in an air oven at 225°F until tacky - approximately 20 minutes.

(7) The sheets are then laid up with a cross bead of undiluted adhesive mixture between each layer.

(8) The laminate package is then evacuated to less than 200 microns for 20 minutes without applying any pressure to the laminate.

(9) Pressure is slowly applied to the package and brought up to 200 psi.

(10) Heat is applied to cure the adhesive. Cure conditions used are 1 hour at 180°F followed by a post cure of 1 hour at 300°F.

All laminates subsequent to 40-50B in Table VI were made by this procedure.

7. Mechanical Behavior of Composites

Preparation of Test Specimens

The mechanical properties of the laminated composites were determined by various tests (to be described below). For this, it was necessary to prepare individual specimens of suitable dimensions. After several trials, the following cutting method has been found suitable.

The laminate plate was fixed to a "Transite" (asbestos-cement composition) board with melted beeswax. The desired cuts were made on a "Delta" surface grinder with a 6 inch diamond slitting wheel, 220 grit, rotating at about 3400 rpm. The longitudinal feed rate was about 1 inch per minute. Kerosene spray mist was used as a coolant at first, but "Rust-Lick" G-25-A (a commercial spray coolant) was later substituted to eliminate a possible fire hazard. The cut resulted in smooth edges with no edge cracking visible under optical examination. After cutting, the individual specimens were removed from the "Transite" base by gently warming the wax, and the wax remnants were washed from the specimens with trichloroethylene.

Most of the laminate plates, measuring originally 6 inches x 8 inches and having 20 plies were subdivided as follows:

(1) Four tensile specimens each 0.75 inch uniform width by 6 inches long. Two of these were parallel to the long (8 inch) dimension and two were perpendicular. This was done to test the degree of planar isotropy of the sheet material.

(2) Two compression specimens each 1.50 inch x 1 inch with 80 plies; 1 each, parallel and perpendicular to the long (8 inch) dimension. These had to be relaminated from four primary 20 ply packets to yield compression specimen which would not fail by Euler buckling prior to fracture.

(3) One shear test specimen 1 inch x 0.5 inch with 80 plies relaminated from 4 plate thicknesses, as above, to provide a "short beam" specimen. This type of test was designed to measure the interlaminar shear strength of the composite.

The general cutting schedule is shown schematically in Figure 13. When laminates smaller than 6 inch x 8 inch were produced, the schedule was modified to yield the most information from a smaller number of specimens.

Composite Testing

The mechanical properties of the composite specimens were measured by conventional engineering tests whenever possible.

The methods of test were as follows:

(1) Flexural stiffness: specimens which were 0.75 inch wide, about 0.020 inch thick, and 4 inches or more long, were tested in three-point beam flexure. The flexural modulus of elasticity (E_F) for the composite was computed from elementary beam theory according to

$$E_F = \frac{PL^3}{4Dwt^3} \qquad (2)$$

where
- P = the load applied at the "beam" midspan
- D = the associated midspan deflection
- L = the full "beam" span = 2.25 inches
- w = the specimen width
- t = the specimen thickness

The fixture used for the three-point beam flexure test is shown in Figure 14.

An improved testing jig which provided for four-point bending with beam curvature measurements was designed and

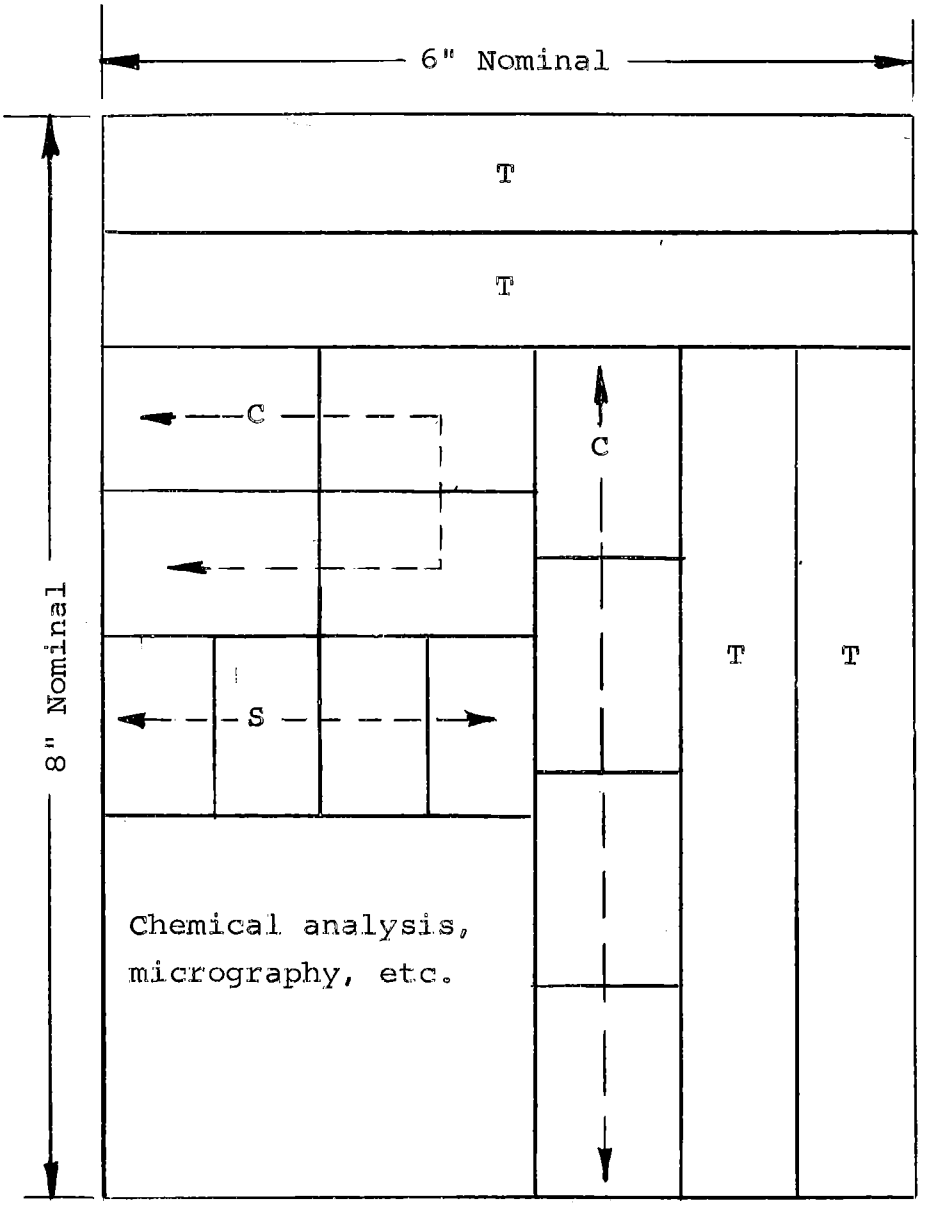

Figure 13

General Cutting Schedule for Boron Carbide Laminates (Not to Scale)

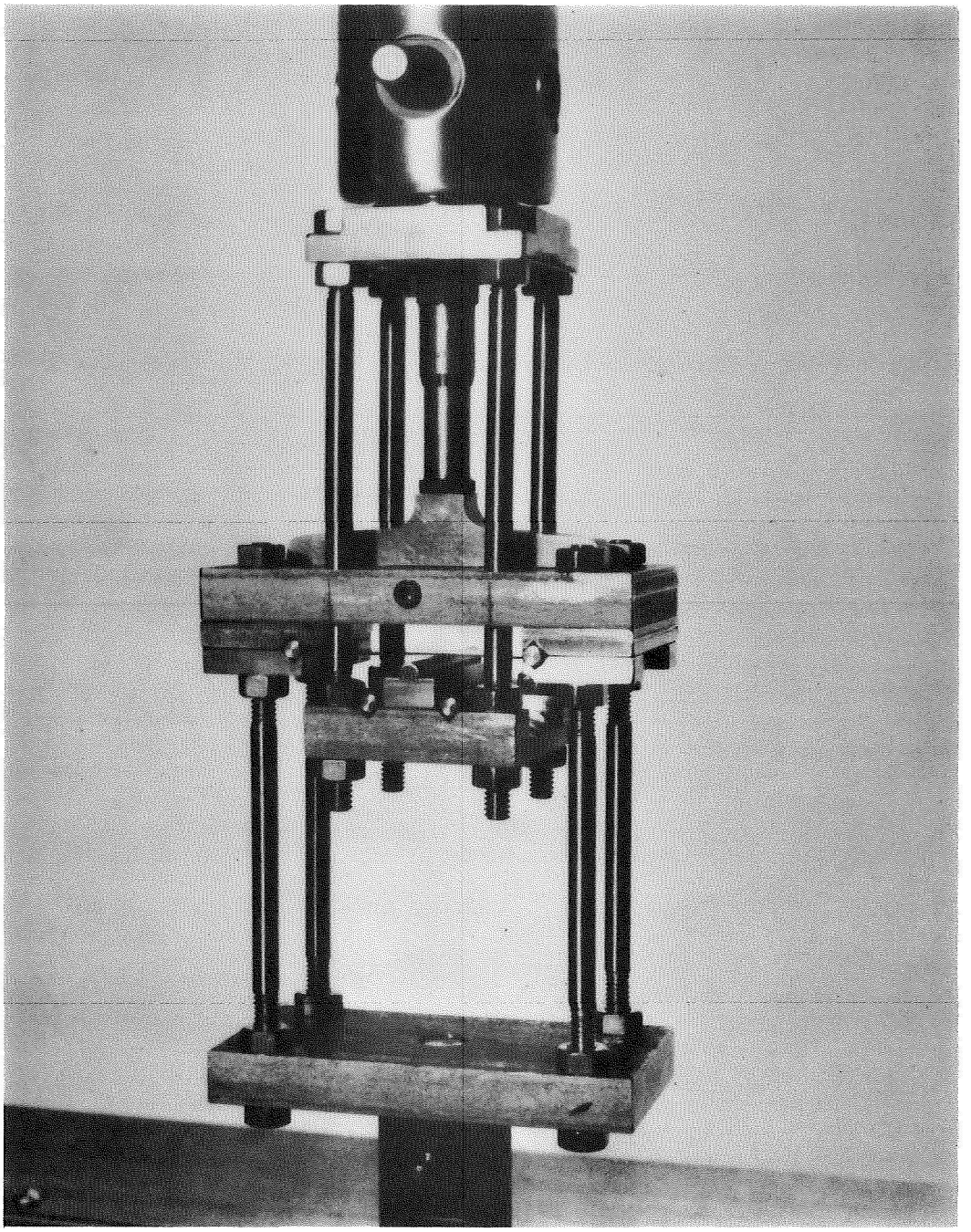

Figure 14

Fixture for the 3-Point Beam Flexure Test

built, and is shown in Figure 15a (front view) and 15b (rear view). Since no shear displacements occur in four-point bending, a possible source of error was eliminated with this method. Only several of the later specimens were tested for flexural stiffness by four-point beam bending.

(2) Tensile modulus: this was derived from the initial slope of the stress-strain curve generated in uniaxial tension tests. Strain was measured with a resistance strain gage extensometer (1 inch gage length) fastened at mid-length of the tensile specimens, or, in most cases, with SR-4 strain gages mounted directly on the specimen surfaces. Such strain gages were used pairwise in order to compensate for any bending components. Elastic displacements of the testing machine and in the tensile grips did not interfere with the strain measurements by either method.

(3) Tensile strength: tests to determine the ultimate strength in uniaxial tension of specimens 0.75 inch wide, about 0.020 inch thick and about 6 inches long were made. The tensile specimens had a uniform cross-section throughout, and were gripped with aluminum cheeks fastened with adhesive at the ends. No lateral pressure was exerted on the specimens; the load transfer was entirely by shear traction. Ball bearing swivels were incorporated into the cross-head and suspension of an Instron testing machine to relieve any initial misalignment and excentric loading. The experimental set-up is illustrated in Figure 16; an "exploded view" close-up of the ball bearing swivel shackle is given in Figure 17. Figure 18 shows the hyperbolically tapered profile of the aluminum gripping cheeks, and a typical fracture in mid-gage length of a tensile specimen. Specimens fractured at or near the middle of the gage length with no exceptions. Load/strain curves for each test were generated by simultaneously plotting the output

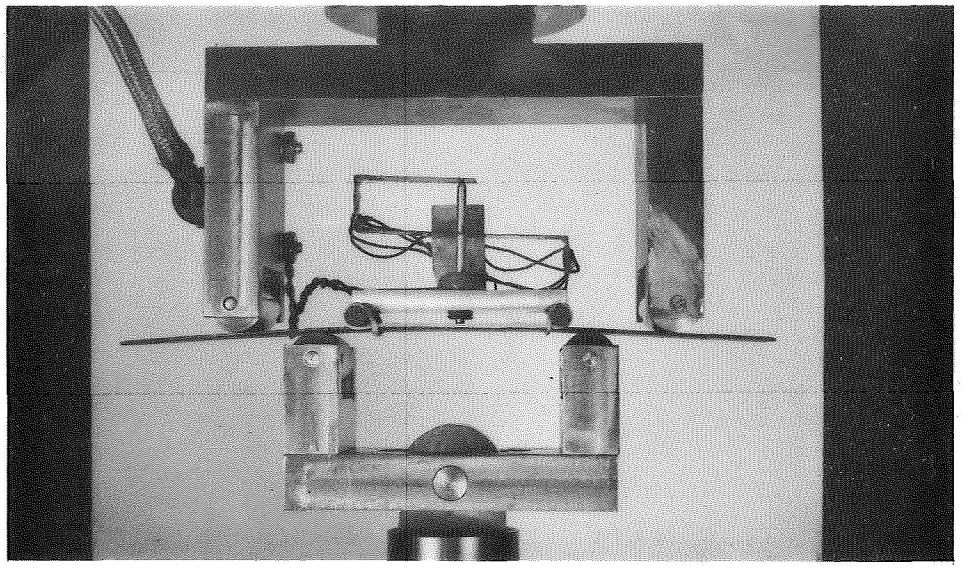

Figure 15a

Four-Point Beam Flexure Test (front view)

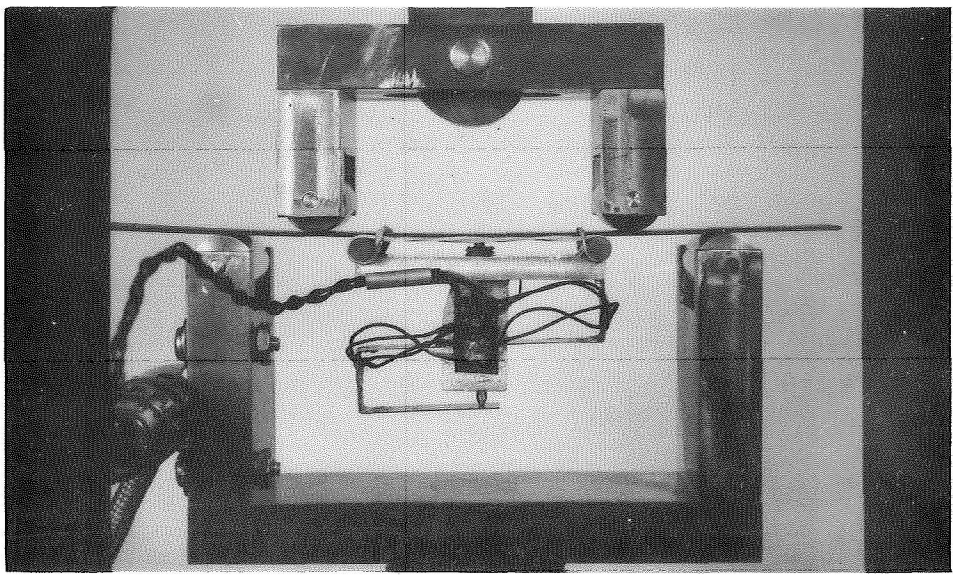

Figure 15b

Four-Point Beam Flexure Test (rear view)

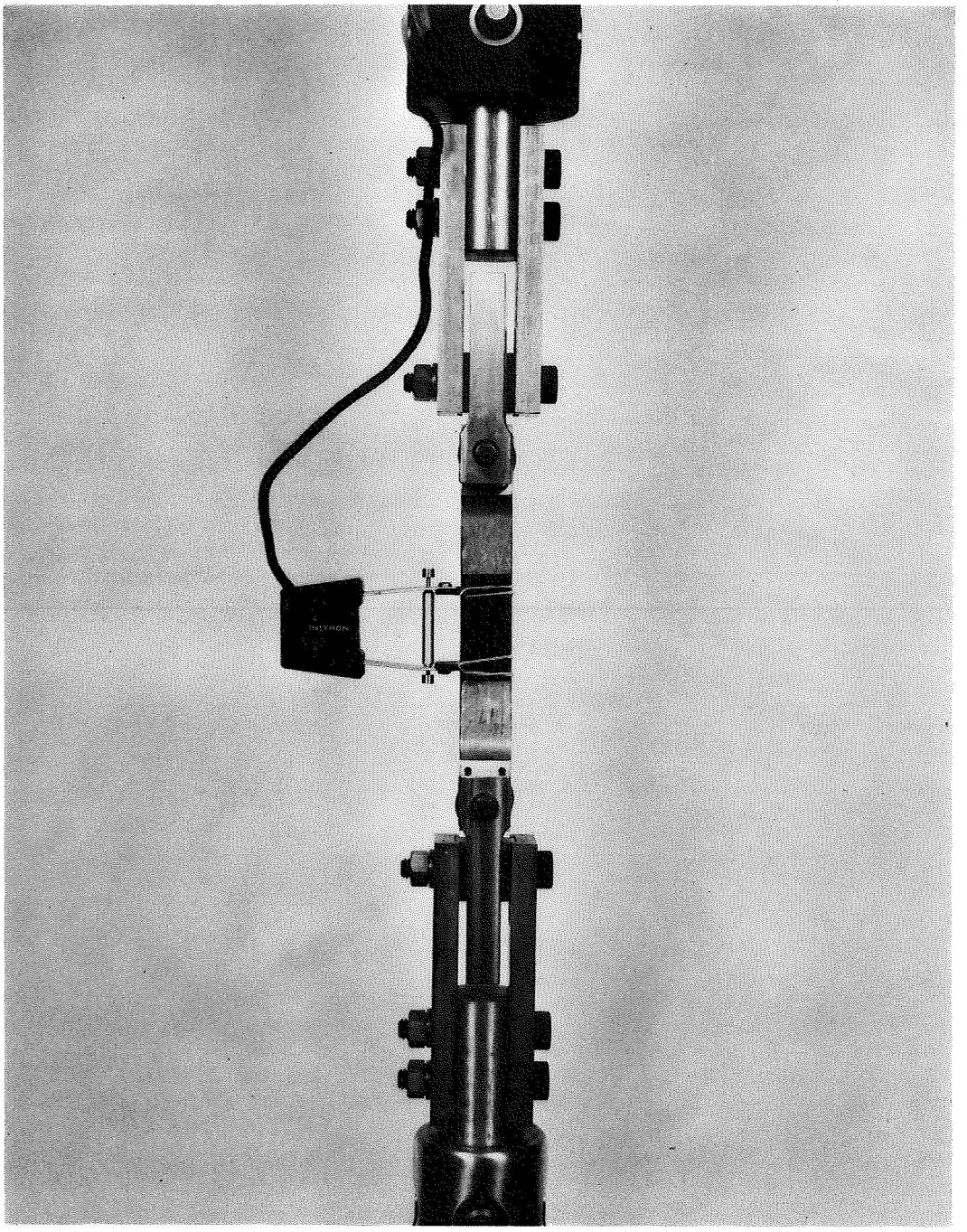

Figure 16

Experimental Set-Up for Tensile Tests

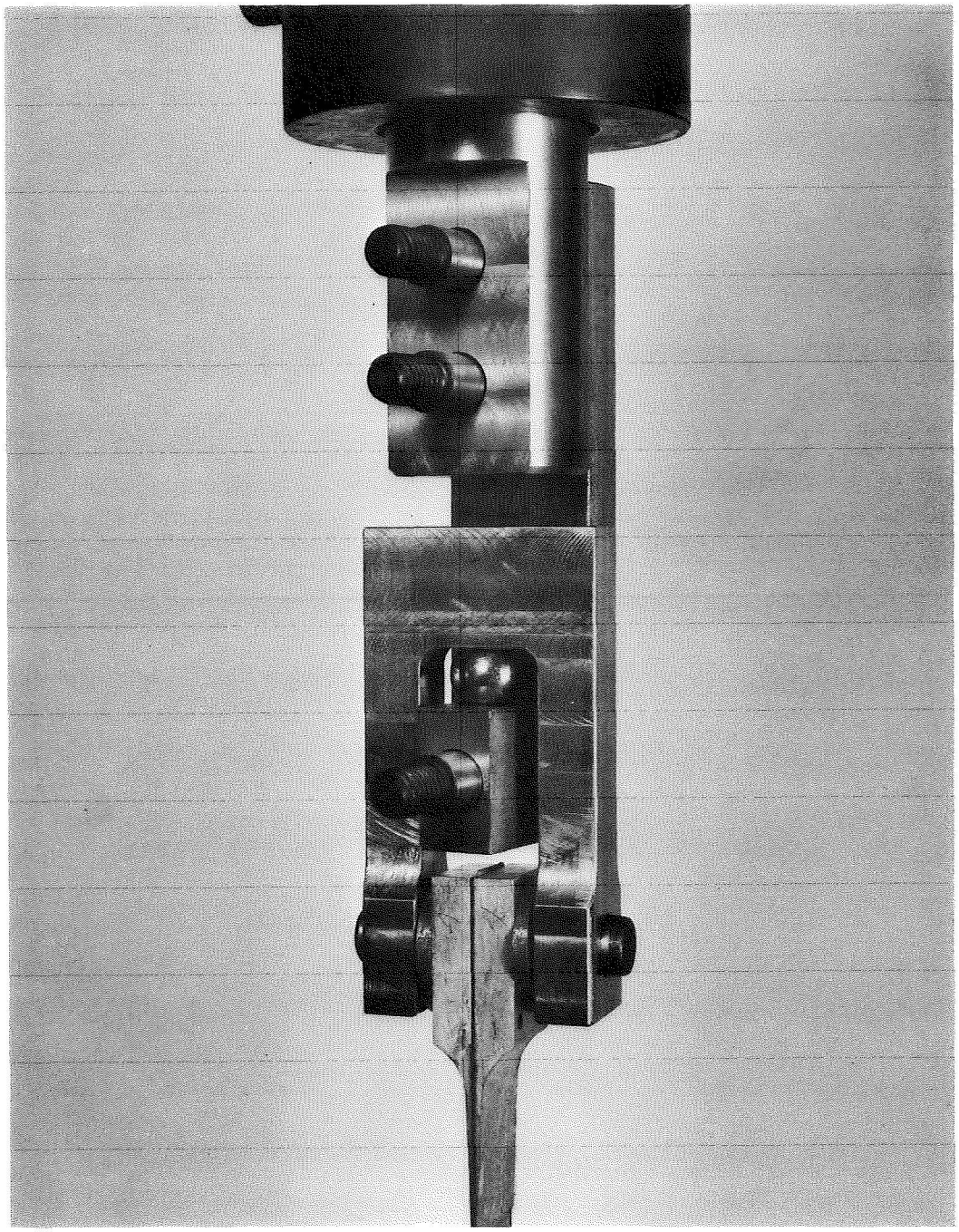

Figure 17

Exploded Close-Up View of Ball Bearing
Swivel Shackle

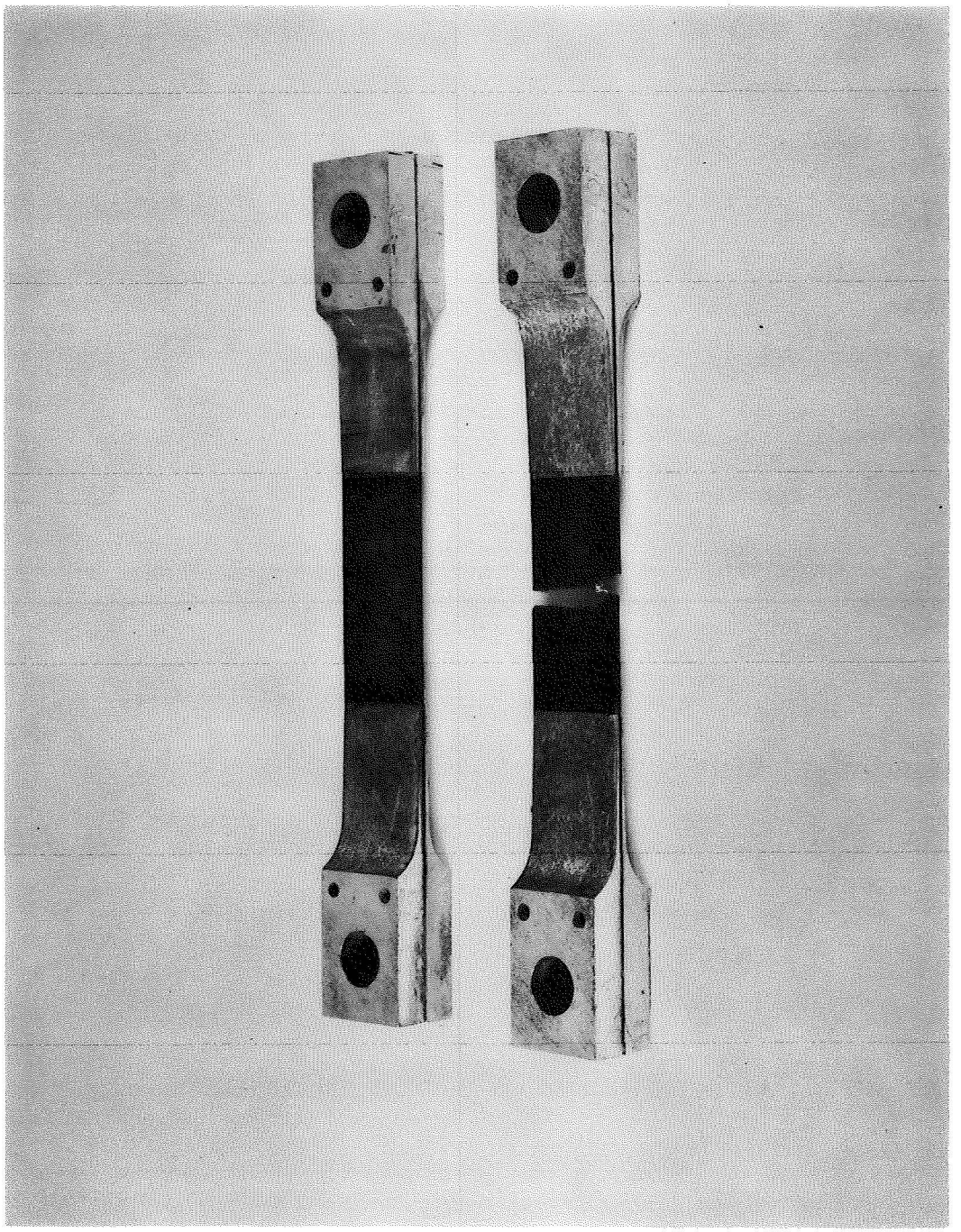

Figure 18

Close-Up of Aluminum Gripping Cheeks for
Tensile Specimens
(Typical Mid-Specimen Fracture Shown)

signals from the Instron load cell and from the strain gages on an X-Y recorder. Continuous curves from the initial linear rise, through the apparently "plastic" range, to the point of fracture, were obtained and converted to "engineering" stress/strain curves by dividing all values of load by the initial cross-sectional area.

A typical stress/strain curve is shown in Figure 19 to illustrate the definitions of the following parameters:

E_T = tensile modulus of elasticity
σ_{pl} = apparent proportional limit stress
σ_U = ultimate strength in tension
ϵ_{pl} = proportional limit strain
ϵ_f = strain at failure
β = post-elastic stress increment

The significance of these parameters is discussed later.

For several of the specimens, the ultimate flexural strength (σ_F) was measured by loading specimens in three-point beam flexure as described above for the flexural stiffness test, but continuing the loading until the "beam" specimens failed by tensile fracture in the mid-span section. The ultimate flexural strength (σ_F) was computed by

$$\sigma_F = \frac{3\ PL}{2\ wt^2} \qquad (3)$$

where P = the maximum mid-span load
L = the "beam" span = 2.25 inch
w = the specimen width
t = the specimen thickness

(4) Compressive strength: for the compressive test, four composite plate thicknesses were relaminated to yield a

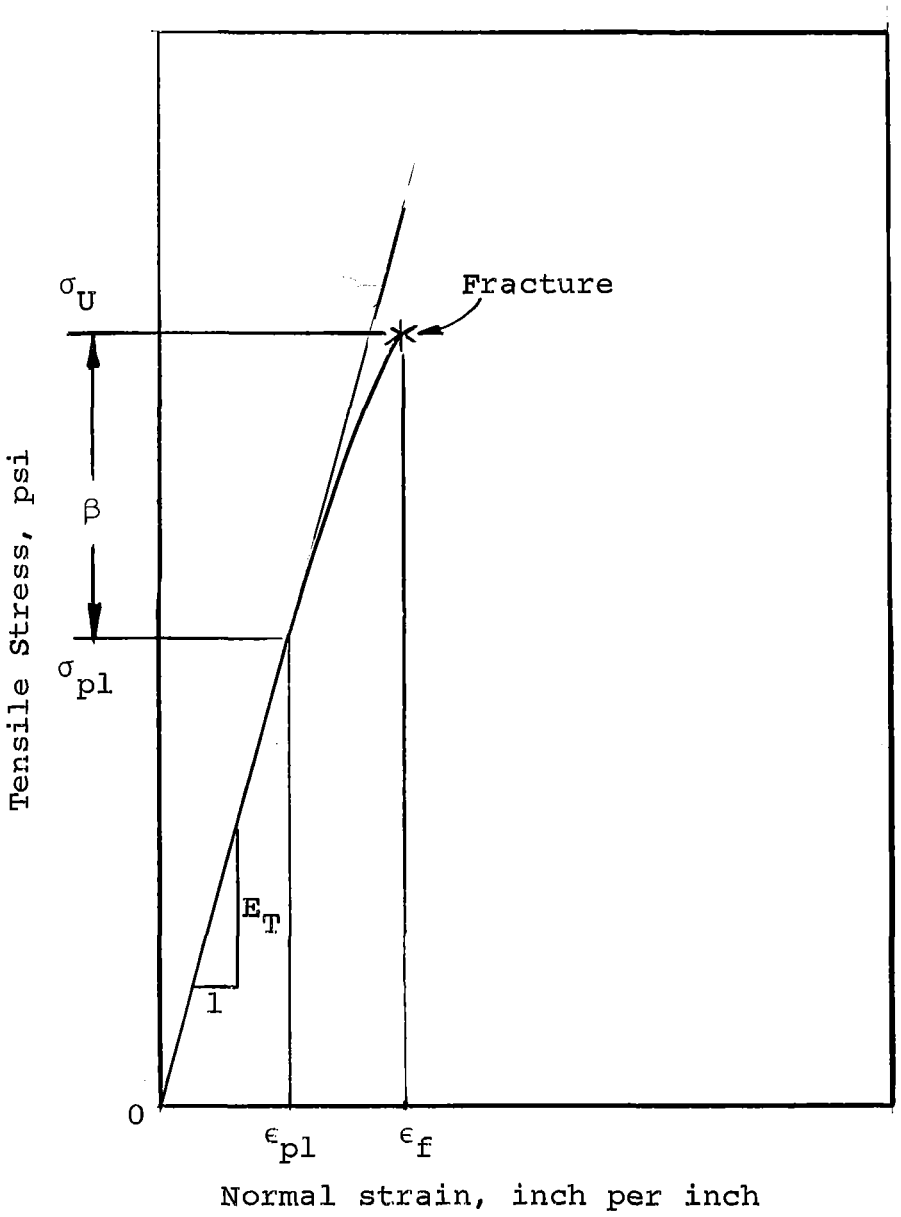

Figure 19

Typical Stress-Strain Curve for Composite Tensile Specimens, With Definitions of Elastic and Post-Elastic Parameters

short column specimen 1.50 inch long, 1 inch wide, and about 0.080 inch thick. The specimen was held in a compression jig such that the column ends could be considered "fixed". The experimental set-up is shown in Figure 20.

(5) Interlaminar shear strength: the test set-up for interlaminar shear strength is shown in Figure 21. Shear test specimens had the dimensions 1 inch x 0.5 inch x approximately 0.080 inch. They were designed as thick, short beams subject to flexure. According to current practice, the maximum load P was recorded and the maximum shear strength was computed by

$$\tau_{max} = \frac{3P}{4A_o} \qquad (4)$$

where P = maximum load before failure

A_o = cross-sectional area

Specimens were examined microscopically to determine the mode of failure. If failure by any mechanism other than shear was observed, the value of τ_{max} was a lower bound and the true interlaminar shear strength was higher.

(6) Shear stiffness test: several attempts were made to measure the shear stiffness (or modulus of rigidity), G, of composite specimen plates by the "saddle bend test", after T. S. Tsai.[8] The resultant shear stiffness values, G, appeared to be nearly equal to the previously measured bending modulus, E. This spurious effect was believed to be due to the inherent geometric instability of Tsai's "saddle" configuration in which the specimen has a strong tendency to snap over into one of two possible configurations of cylindrical curvature. This has been discussed in detail by R. L. Foye.[9] In order to obtain a more reliable measure for the shear

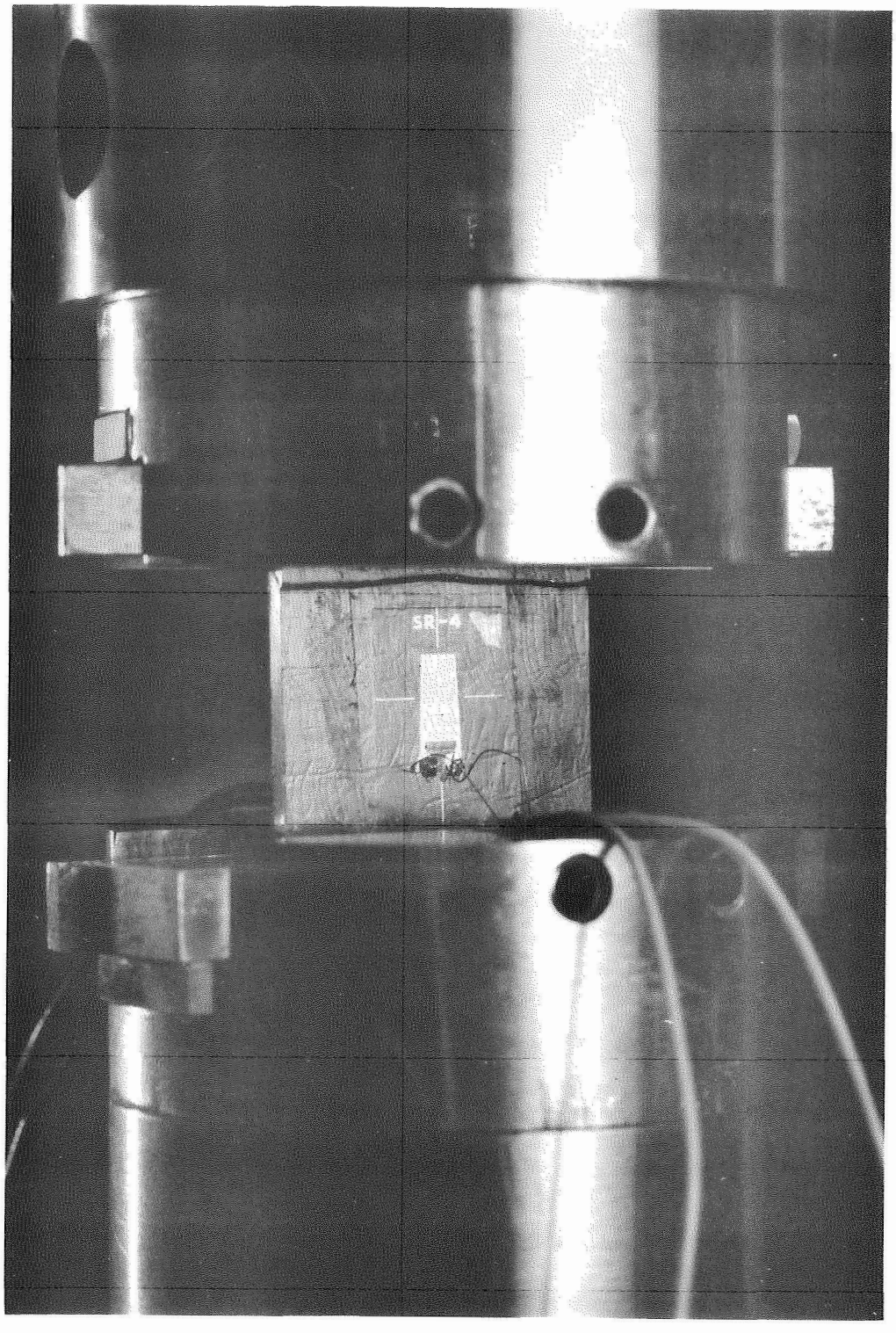

Figure 20

Experimental Set-Up for Compression Tests

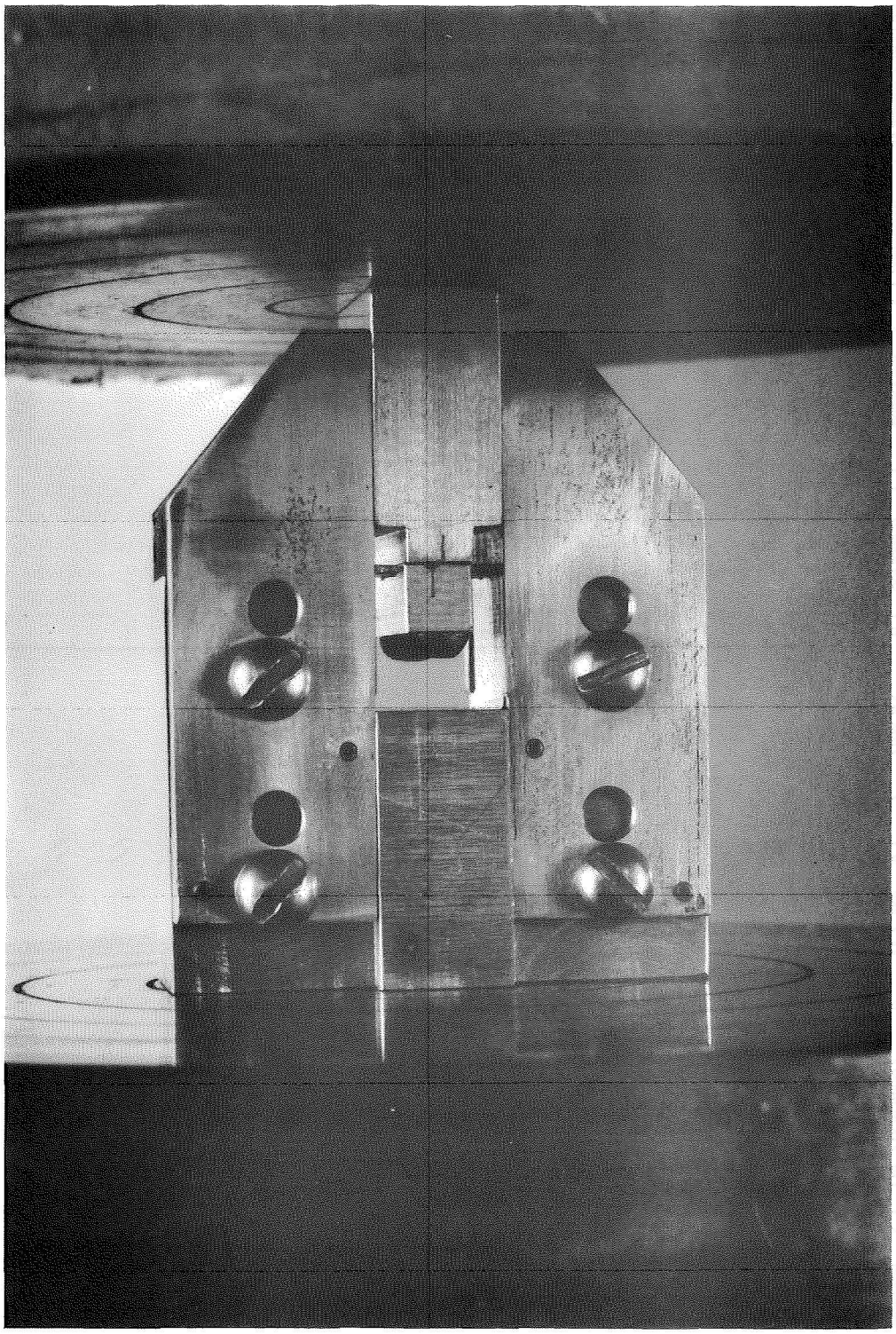

Figure 21

Experimental Set-Up for Interlaminar
"Short Beam" Shear Test

modulus, G , a very simple torque/twist device was designed and built. It is illustrated in Figure 22. The shear modulus G for some of the later specimens was measured, and computed by

$$G = \frac{3TL}{wt^3 \theta} \qquad (5)$$

where
- T = applied torque (inch pounds)
- L = specimen length between slotted grips (inches)
- w = specimen width (inches)
- t = specimen thickness (inches)
- θ = angle of twist (radians)

(7) Weight density: rectangular pieces, approximately 1/2 inch square, were cut from the specimen plates at the conclusion of the tests, and the weight-density was determined by gravimetric means. The weight-density, ρ , was computed by

$$\rho = \frac{M}{a \cdot b \cdot t} \qquad (6)$$

where
- M = sample weight (pounds)
- a = sample length (inches)
- b = sample width (inches)
- t = sample thickness (inches)

Experimental Results

All quantitative results obtained from the mechanical tests have been listed in Tables VII - XI. The laminates contained boron carbide film reinforcement varying from 10.9 to 27.3 volume percent and the fractional content is shown

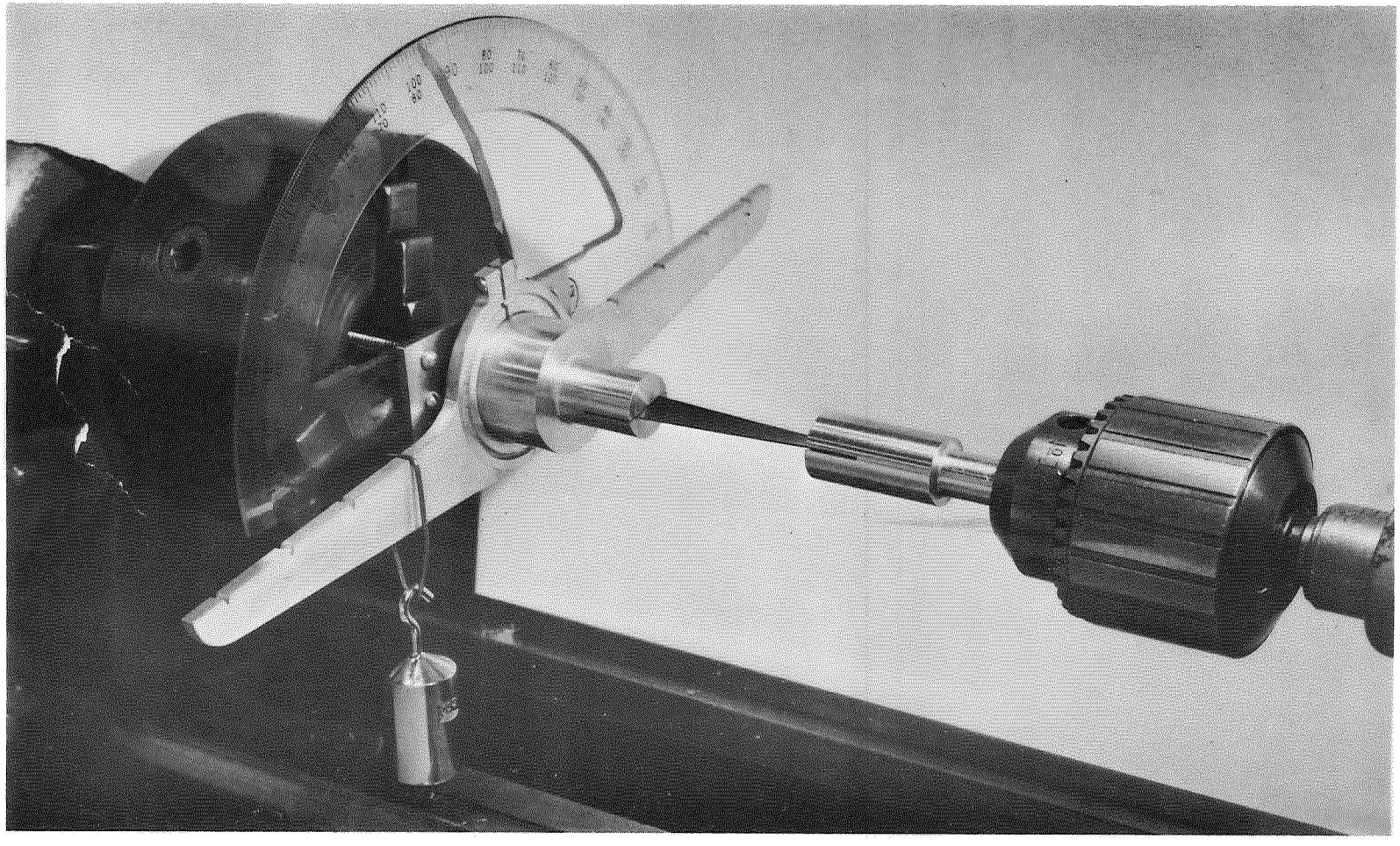

Figure 22

Simple Torque/Twist Device
to Measure Modulus of Rigidity, G

(to the nearest 0.1%) in the first column of the tables. In the case of compression and shear specimens, the volume fraction of reinforcement was usually lower than that shown for the corresponding tensile specimens, since relamination to 80-ply thickness added three extra adhesive layers. Results for aluminum substrate and for Kapton substrate composites have been listed separately, and the type of adhesive used (phenoxy or epoxy) has also been indicated by separate subheadings.

Values for the modulus of elasticity E are listed in Table VII where separate columns are used to show the flexural, tensile, and compressive moduli (E_F, E_T, and E_C respectively). All flexural moduli (E_F) shown in Table VII were measured by the three-point beam flexure test, except for a small number of specimens which were also tested in four-point beam flexure.

The modulus of rigidity (G) is listed in Table VIII for the more recent specimens for which the torque/twist test has been performed.

Data for the proportional limit stress (σ_{pl}) (where available), and for the ultimate strength of laminates are shown in Table IX with separate columns assigned for ultimate uniaxial tensile strength (σ_U), free column compressive strength (σ_C), and ultimate flexural strength (σ_F).

The interlaminar shear strength (τ_{max}) as determined by the short beam shear test has been listed in Table X.

The weight-density, together with the computed values of specific flexural modulus (E_F/ρ) and specific tensile strength (σ_U/ρ) are listed in Table XI. Only the maximum value for each laminate plate has been shown in this table.

TABLE VII

Modulus of Elasticity of Boron Carbide Reinforced Laminar Composites

Specimen No.	Volume fraction boron carbide (%)	Flexural modulus E_F (10^6 psi) (a)	Tensile modulus E_T (10^6 psi) (b)	Compressive modulus E_C (10^6 psi) (c)
Aluminum Foil Substrate, Epoxy Adhesive				
40-69A	16.8	12.7	8.7	
B	↓	11.3	8.2	
C		9.3	---	
D		10.4	---	
40-90A	21.8	17.1 20.8 (d)	16.9	
Kapton Film Substrate, Phenoxy Adhesive				
2848-14A	18.9	7.8	6.6	---
B	↓	8.4	6.1	---
C		9.3	9.2	---
D		8.4	7.3	---
E	16.3	---	---	8.2
F	18.1	---	---	7.1
2808-15A	10.9	5.0	5.0	---
B		6.4	4.6	---
C		6.1	6.5	---
D		6.7	4.9	---
E		---	---	5.9
Kapton Film Substrate, Epoxy Adhesive				
2844-17A	18.6	---	8.4	---
B	↓	8.9	9.8	---
C		9.3	8.5	---
2848-20A	16.3	8.3	6.4	---
B		8.9	8.8	---

con't.....

Modulus of Elasticity of Boron Carbide Reinforced Laminar Composites

Specimen No.	Volume fraction boron carbide (%)	Flexural modulus E_F (10^6 psi) (a)	Tensile modulus E_T (10^6 psi) (b)	Compressive modulus E_C (10^6 psi) (c)
Kapton Film Substrate, Epoxy Adhesive - Concluded				
2848-26A	14.5	8.7	7.1	---
B	↓	9.9	7.3	---
C	↓	9.0	7.5	---
2844-25A	25.6	8.6	6.9	---
B	↓	8.7	7.9	---
2848-28A	18.1	8.1	7.1	---
B	↓	7.7	5.8	---
C	↓	10.0	8.9	---
D	↓	9.1	8.7	---
E	15.5	---	---	8.4
F	16.2	---	---	8.6
40-42A	27.3	14.7 (d) 16.4 (d)	13.6	---
B	↓	13.4	---	---
E	26.5	---	---	13.6
40-47A	24.0	10.6 (d) 12.0 (d)	9.8	---
B	↓	10.1	---	---
E	23.4	---	---	11.9
40-72A	17.5	9.4	5.6	---
B	↓	8.6	5.9	---
C	↓	9.7	---	---
D	↓	9.6	---	---

[a]Three-point beam flexure test, except as noted.

[b]Uniaxial tension test.

[c]Uniaxial compression test.

[d]Four-point beam flexure test.

TABLE VIII

Modulus of Rigidity G of Boron Carbide Reinforced Laminar Composites

Specimen No.	Volume fraction boron carbide %	Modulus of rigidity, G 10^6 psi (a)
Aluminum Foil Substrate, Epoxy Adhesive		
40-69A	16.8	7.1
B	↓	5.7
C		6.4
D		4.1
40-90A	21.8	6.9
Kapton Film Substrate, Epoxy Adhesive		
40-72A	17.5	6.1
B	↓	5.9
C		5.8
D		5.8

[a]Measured by torque/twist test.

TABLE IX

Strength Properties of Boron Carbide Reinforced Laminate Composites

Specimen No.	Volume fraction boron carbide (%)	Proportional limit stress (10^3 psi) σ_{pl}	Ultimate tensile strength (10^3 psi) σ_U (a)	Ultimate flexural strength (10^3 psi) σ_F (b)	Ultimate compressive strength (10^3 psi) σ_C (c)
Aluminum Foil Substrate, Epoxy Adhesive					
40-69A	16.8	3.5	14.7	--	--
B	↓	4.1	16.3	--	--
C		--	--	34.0	--
D		--	--	34.5	--
40-90A	21.8	7.6	19.8	--	--
Kapton Film Substrate, Phenoxy Adhesive					
2848-14A	18.9	5.8	13.8	--	--
B	↓	5.6	14.6	--	--
C		6.0	17.0	--	--
D		11.0	14.3	--	--
E	16.3	--	--	--	22.0 (d)
F	18.1	--	--	--	14.9 (d)
2808-15A	10.9	--	17.5	--	--
B	↓	--	14.6	--	--
C		--	17.5	--	--
D		--	16.3	--	--
E		--	--	--	38.0
Kapton Film Substrate, Epoxy Adhesive					
2844-17A	18.6	--	18.7	--	--
B	↓	--	18.5	--	--
C		--	19.5	--	--
2848-20A	16.3	--	19.0	--	--
B	↓	--	22.4	--	--

con't....

Strength Properties of Boron Carbide Reinforced Laminate Composites

Specimen No.	Volume fraction boron carbide (%)	Proportional limit stress (10^3psi) σ_{pl}	Ultimate tensile strength (10^3psi) σ_U (a)	Ultimate flexural strength (10^3psi) σ_F (b)	Ultimate compressive strength (10^3psi) σ_C (c)
Kapton Film Substrate, Epoxy Adhesive - Concluded					
2848-26A	14.5	--	18.1	--	--
B	↓	--	17.7	--	--
C	↓	--	18.1	--	--
2844-25A	25.6	--	13.6	--	--
B	↓	7.2	15.0	--	--
2848-28A	18.1	11.5	18.2	--	--
B	↓	11.6	16.7	--	--
C	↓	16.4	21.4	--	--
D	↓	14.9	19.3	--	--
E	15.5	--	--	--	37.0
F	16.2	--	--	--	39.0
G	15.5	--	--	--	34.1
40-42A	27.3	22.0	28.3	--	--
B	↓	--	--	57.4	--
E	26.5	53.4	--	--	53.4
40-47A	24.0	18.7	25.8	--	--
B	↓	--	--	53.2	--
E	23.4	--	--	--	57.2
40-72A	17.5	13.9	21.4	--	--
B	↓	16.1	21.5	--	--
C	↓	--	--	54.3	--
D	↓	--	--	54.3	--

[a]Uniaxial tension test.

[b]Three-point beam flexure test.

[c]Fixed-ended, short column compression test. No lateral supports.

[d]Premature failure by delamination.

TABLE X

Interlaminar Shear Strength of
Boron Carbide Reinforced Laminar Composites

Specimen No.	Volume fraction boron carbide %	Interlaminar shear strength, τ_{max} 10^3 psi (a)	Observed mode of failure
Aluminum Foil Substrate, Epoxy Adhesive			
40-69E	16.5	5.3	Tensile failure
F	16.2	6.4	Tensile failure
Kapton Film Substrate, Phenoxy Adhesive			
2808-15G	10.8	4.6	Shear failure
Kapton Film Substrate, Epoxy Adhesive			
2848-28A	15.8	3.7	Shear and tensile failure
I	16.9	4.2	Tensile failure
40-42C	25.5	4.9	Tensile failure
40-47C	23.4	4.8	Tensile failure
40-72E	17.3	6.7	Shear failure
F	16.8	6.4	Tensile failure

[a]When any mode of failure other than transverse de-cohesion of laminae was observed, the actual shear strength was greater than the value shown. In that case, τ_{max} is a lower bound.

TABLE XI

Density and Weight - Specific Mechanical Properties of Boron Carbide Reinforced Laminar Composites

Laminate No.	Vol. Fraction Boron Carbide %	Density pci	Specific Flexural Modulus 10^8 inch	Specific Tensile Strength 10^5 inch
Aluminum Foil Substrate, Epoxy Adhesive				
40-69	16.8	.089	1.43	1.83
40-90	21.8	.085	2.02	2.33
Kapton Film Substrate, Phenoxy Adhesive				
2848-14	18.9	.054	1.72	3.15
2808-15	10.9	.052	1.29	3.37
Kapton Film Substrate, Epoxy Adhesive				
2844-17	18.6	.049	1.90	3.98
2848-20	16.3	.058	1.53	3.86
2848-26	14.5	.062	1.60	2.92
2844-25	25.6	.048	1.82	3.13
2848-28	18.1	.057	1.75	3.76
40-42	27.3	.056	2.63	5.06
40-47	24.0	.050	2.12	5.16
40-72	17.5	.057	1.70	3.78

Discussion of Results

Stiffness

The measured stiffness for all Kapton substrate specimens has been plotted versus volume percent boron carbide in Figure 23. Aluminum substrate specimens have been excluded in this plot. The dashed line represents 100% effectiveness of the reinforcement, i.e., the theoretical composite stiffness as predicted by the Rule-of-Mixtures. Dotted lines representing 80, 60 and 40% effectiveness of the reinforcement are also shown.

The measured values of the elastic moduli depended on the method of test. The four-point beam flexure tests consistently indicated the highest apparent stiffness, while the three-point beam flexure tests indicated somewhat lower numbers. Tensile and compressive modulus values appeared to be lower still, in general.

Two or three specimens had a stiffness exceeding the Rule-of-Mixtures prediction, i.e., appeared to be more than 100% effective. The average effectiveness of the reinforcement appeared to be about 80%. No correlation between reinforcement effectiveness and any of the fabrication parameters could be established, but in general, the laminates fabricated towards the end of the program had the higher effectiveness.

Tensile Strength

The strength of the reinforcement phase could not be deduced unambiguously from the observed composite stress-strain behavior. Up to the proportional limit (σ_{pl}), homogeneous strains in the constituents were assumed, and the stiff phase could be said to carry essentially all of the load. Once the stress-strain curve departed from the initial tangent line, however, the relative contributions to the

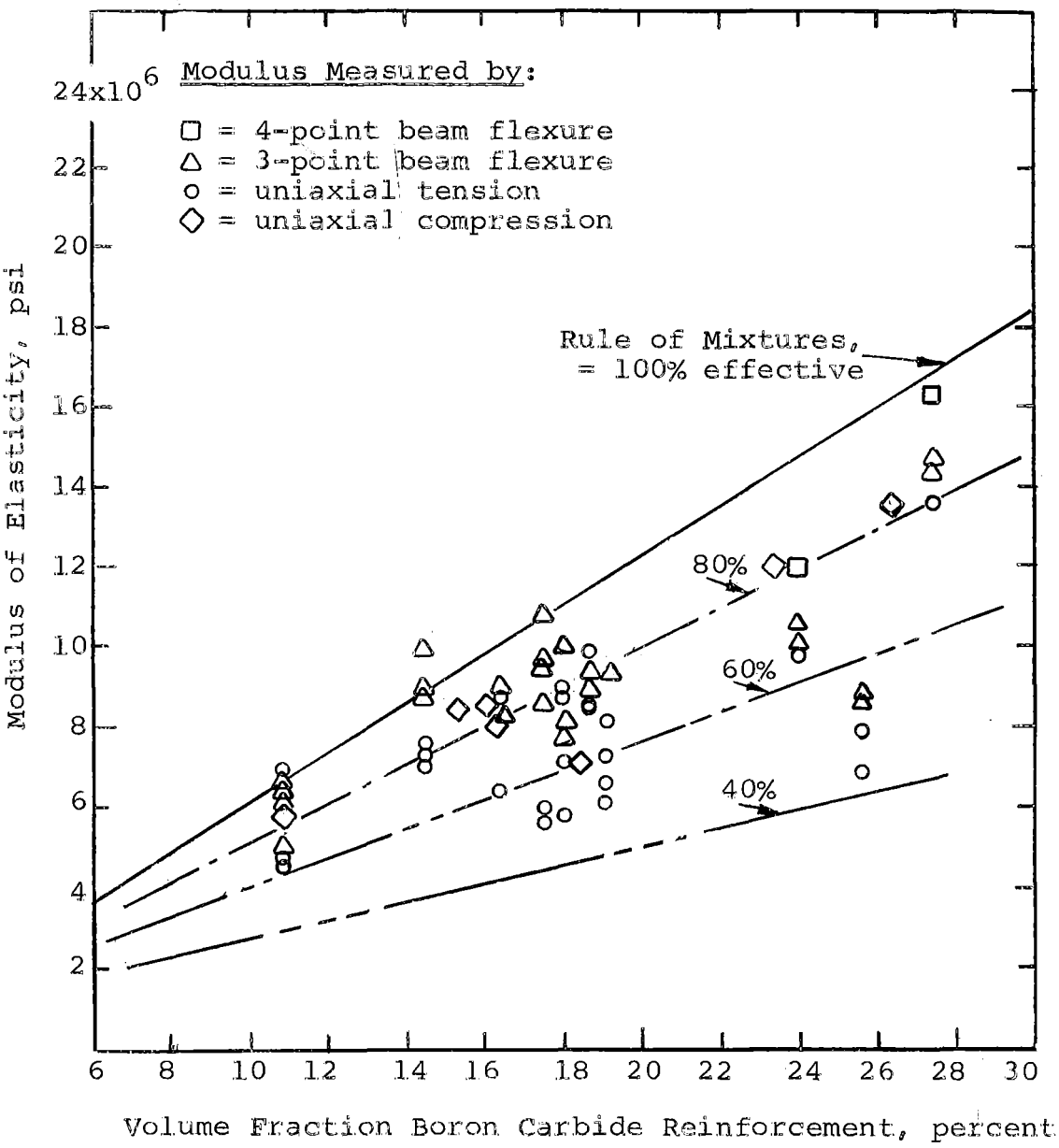

Figure 23

Elastic Modulus of Boron Carbide (Kapton Substrate) Composite Specimens as a Function of the Volume Fraction of Reinforcement. Modulus Measured by Different Methods of Test.

tensile strength by the several phases was indeterminate. It is known that boron carbide does not behave plastically, so that any irreversible "plastic" strain in the composite must have been due to the softer matrix. Plastic behavior in the matrix could occur in local regions of reinforcement fracture, or in the vicinity of geometric defects where, for example, the initial lay-up of the reinforcement sheets was not strictly planar. The higher failure stress (σ_U) therefore most likely reflected the ultimate strength of the matrix, since the reinforcement must have failed internally over significant regions of the laminate once the proportional limit stress was exceeded.

The critical stress (σ_{cr}) in the reinforcement, i.e., the stress level at which local failures in the boron carbide will occur, can be computed from

$$\sigma_{cr} = \epsilon_{pl} E_r \qquad (7)$$

where ϵ_{pl} = the homogeneous strain in the composite at the proportional limit,

E_r = the Young's modulus of the reinforcement, (taken to be 60×10^6 psi for boron carbide)

This analysis is a conservative one, since neither isolated breaks in the reinforcement, nor non-linear stress-strain behavior necessarily indicate a strength limitation in the engineering sense, provided the ultimate strength of the composite (σ_U) is greater than the proportional limit stress (σ_{pl}) by a suitable margin, and no precipitous loss of stiffness (defined by the tangent modulus) occurs.

A plot of the observed proportional limit stress (σ_{pl}) versus the associated tensile modulus of elasticity (E_T) is

shown in Figure 24. The dashed lines radiating from the origin of the coordinate system are loci of constant proportional limit strain (ϵ_{pl}). Specimens comprising Kapton substrate and epoxy adhesive exhibited proportional limit strains from .0016 to .0027, while the aluminum substrate/epoxy specimens appeared to be grouped in the range $0.0004 < \epsilon_{pl} < 0.0005$. The older Kapton/phenoxy specimens were in the intermediate range $0.0006 < \epsilon_{pl} < .0014$. The corresponding strength of the reinforcement, computed, according to Eq. (7) was,

σ_{cr} = 96 to 162 x 10^3 psi for Kapton/epoxy composites

σ_{cr} = 36 to 90 x 10^3 psi for the older Kapton/phenoxy composites

σ_{cr} = 24 to 30 x 10^3 psi for the aluminum/epoxy composites

In every specimen, the ultimate tensile strength was greater than the proportional limit stress by a considerable margin. This is shown in Figure 25, where the proportional limit stress (σ_{pl}) has been plotted versus the ultimate tensile stress (σ_U). The dashed line through the origin with slope = 1 indicates the limiting behavior for an ideally brittle-elastic material. The observed behavior could be described approximately by

$$\sigma_U = \sigma_{pl} + \beta \qquad (8)$$

where β = a fixed increment, independent of volume fraction

The value of the post-elastic stress increment β was nearly constant at about 6 x 10^3 psi for all Kapton/epoxy

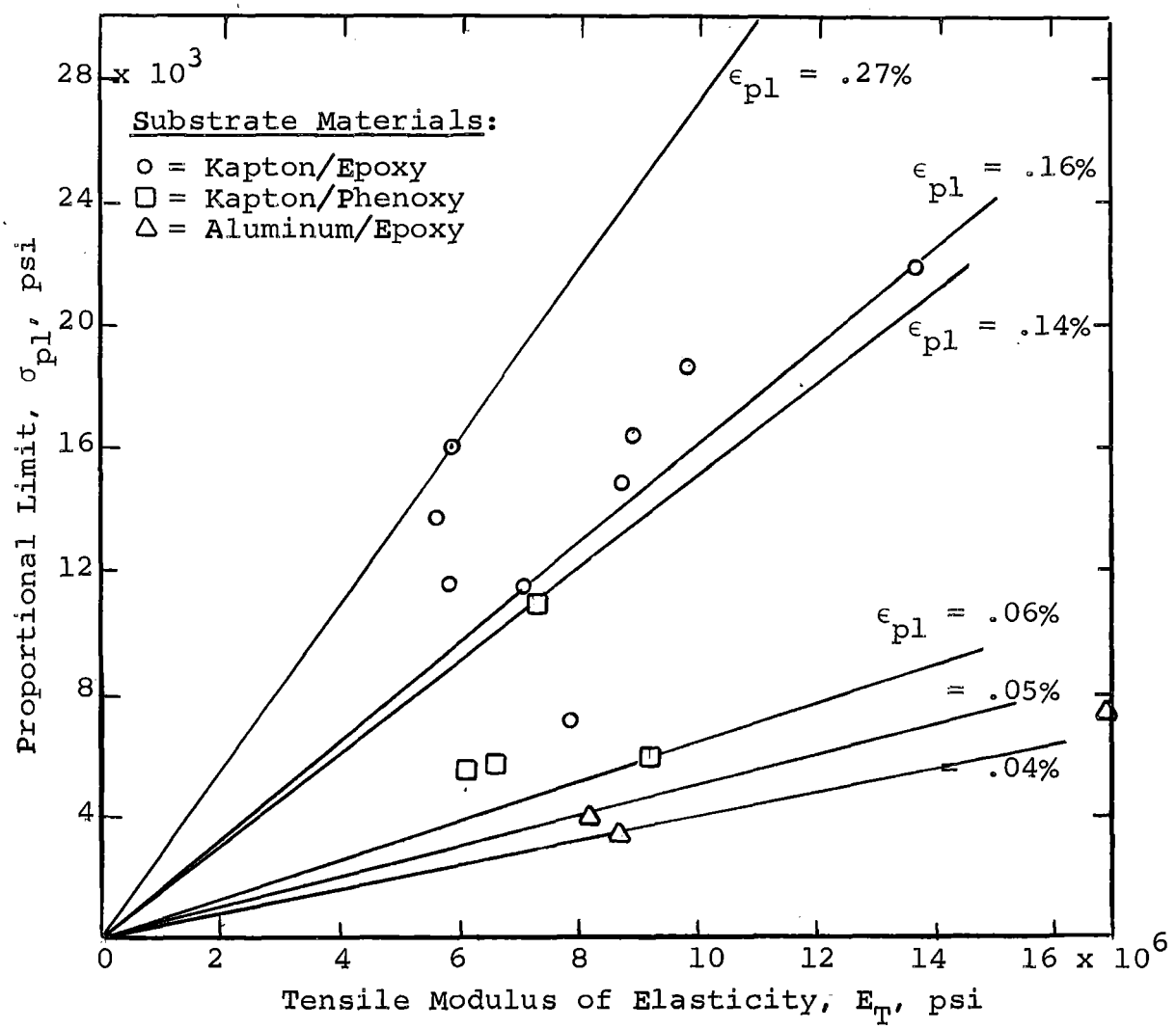

Figure 24

Proportional Limit Stress Vs. Tensile Modulus of Elasticity for Boron Carbide Sheet Composites

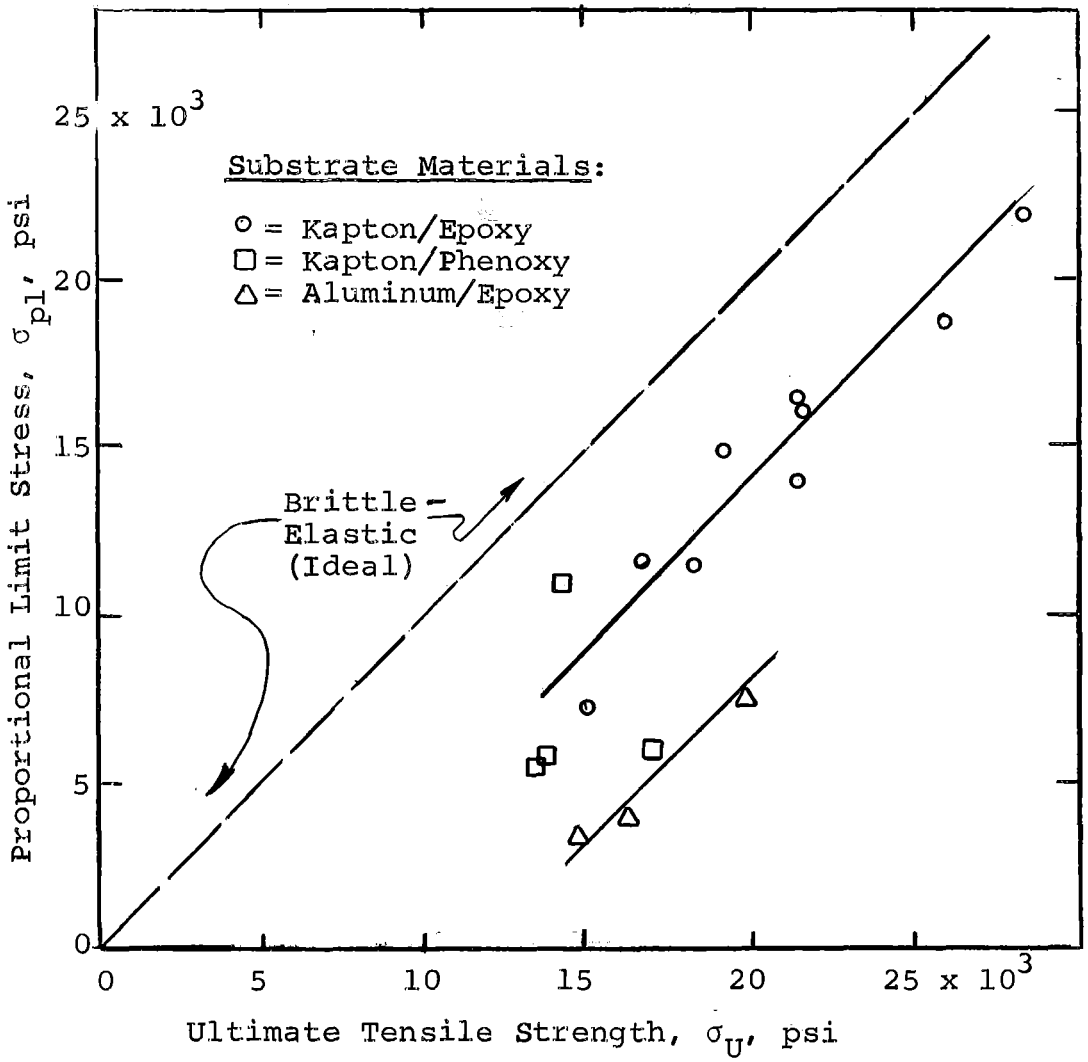

Figure 25

Proportional Limit Stress vs. Ultimate Strength of Boron Carbide Sheet Composites

samples, and about 12 x 10^3 psi for the aluminum/epoxy specimens. For the Kapton/phenoxy specimens, the behavior was much less regular, reflecting the greater uncertainty and variability associated with the earlier, less experienced fabrication methods.

No explanation for the apparent constancy of the post-elastic stress increment β is presently at hand. The dependence of the magnitude of β on the substrate material rather than on the volume fraction or other characteristic of the reinforcement phase, however, supports the initial argument that the reinforcement is most effective only up to the proportional limit. This contention is further supported by the appearance of the plot of ultimate tensile strength (σ_U) versus tensile modulus of elasticity (E_T), Figure 26. On this plot, the ultimate strength of the specimens seems to be very weakly related to the initial elastic behavior, if at all, and no regular grouping of data points according to substrate or adhesive constituents is discernible in this representation.

Flexural Strength

The apparent ultimate flexural strength, σ_F, as tested in three-point beam flexure was consistently higher by a factor of 2 to 3 than the ultimate tensile strength, σ_U, of corresponding specimens. This could be explained by the relatively thin section of the specimens, owing to which they behaved like thin plates rather than "beams". The deflections just before and at bending failure were large enough to cause 30-40° rotations of the specimen logitudinal axis at the supports, such that small deflection beam theory, Eq. (3), should no longer be applied without suitable modifications. Values of σ_F computed by Eq. (3) have been reported nevertheless to permit comparisons with the results which have been published in the current literature.

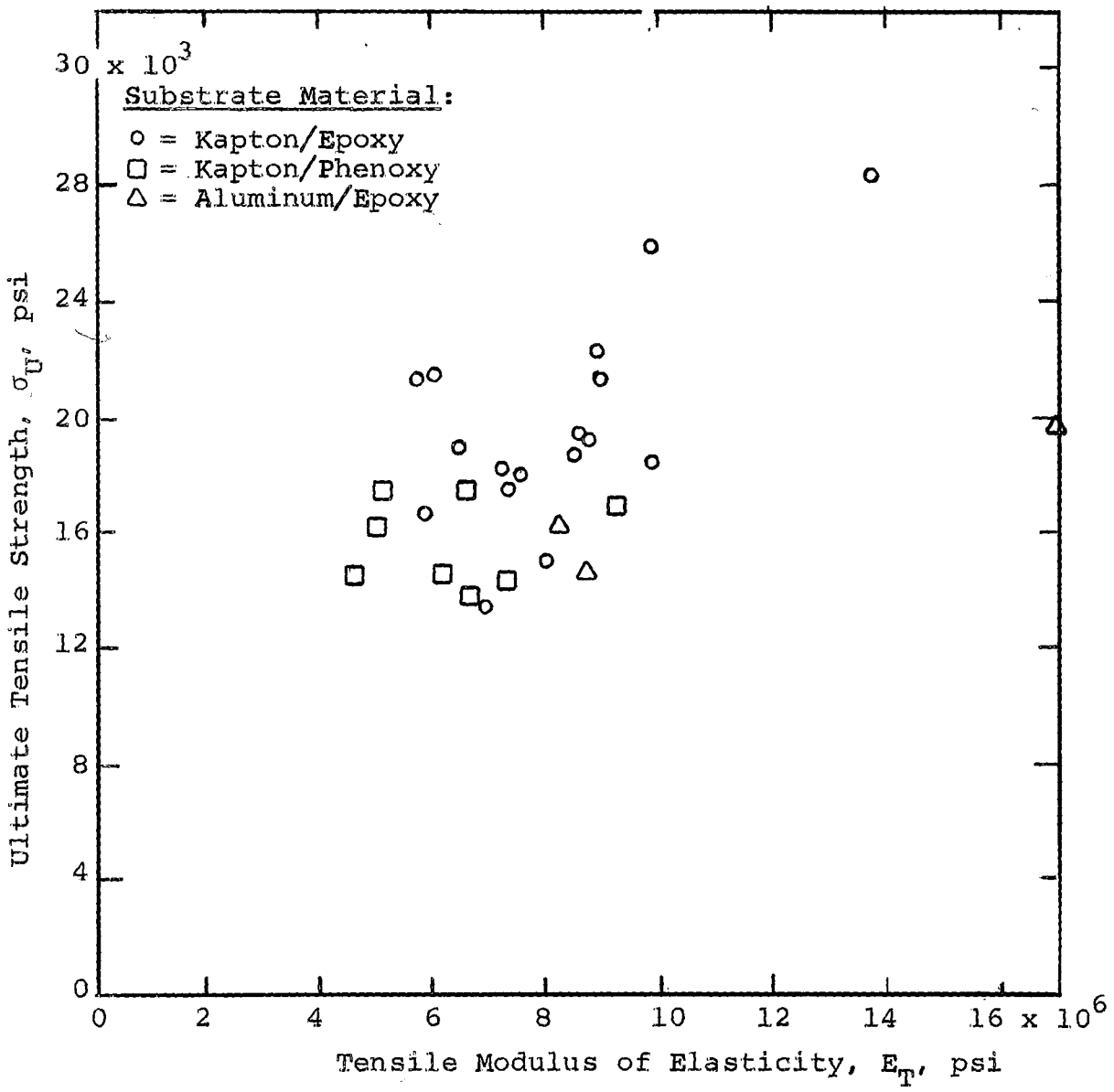

Figure 26

Ultimate Strength vs. Tensile Modulus of Elasticity of Boron Carbide Sheet Composites

Compressive Strength

In most instances (exceptions have been noted in Table IX), the mode of failure consisted of diagonal kinking of individual reinforcement layers. (A similar effect has also been reported for filamentary composite materials, and has been termed "microbuckling".) Several examples of failed compression specimens are shown in Figures 27, 28, and 29.

The ultimate strengths of all the samples tested in compression were higher than the corresponding tensile strengths by a factor of 2 to 3. Since the failure generally was coincident with geometric instability and local buckling, the intrinsic cohesive strength in compression of the material may be much higher than reported.

Interlaminar Shear Strength

Most of the samples tested failed in tension rather than in shear, so that the values of τ_{max} listed in Table X represent a lower bound rather than the true limit of the interlaminar shear strength. In testing certain specimens (not part of this investigation) in which premature tensile failures were prevented by special auxiliary reinforcement arrangements, the same epoxy adhesives applied and cured in the same way had shear strengths on the order of 10×10^3 psi, in agreement with the values often reported by other investigators for boron fiber/plastic matrix composites. Photomicrographs of several failed shear specimens are shown in Figures 30 and 31. It was clear that lack of sufficient interlaminar shear strength was not a problem for the present.

Shear Modulus

The modulus of rigidity, G, of a linear elastic solid is related to two or more (depending on the structural symmetry) of the other elastic constants. For homogeneous, isotropic

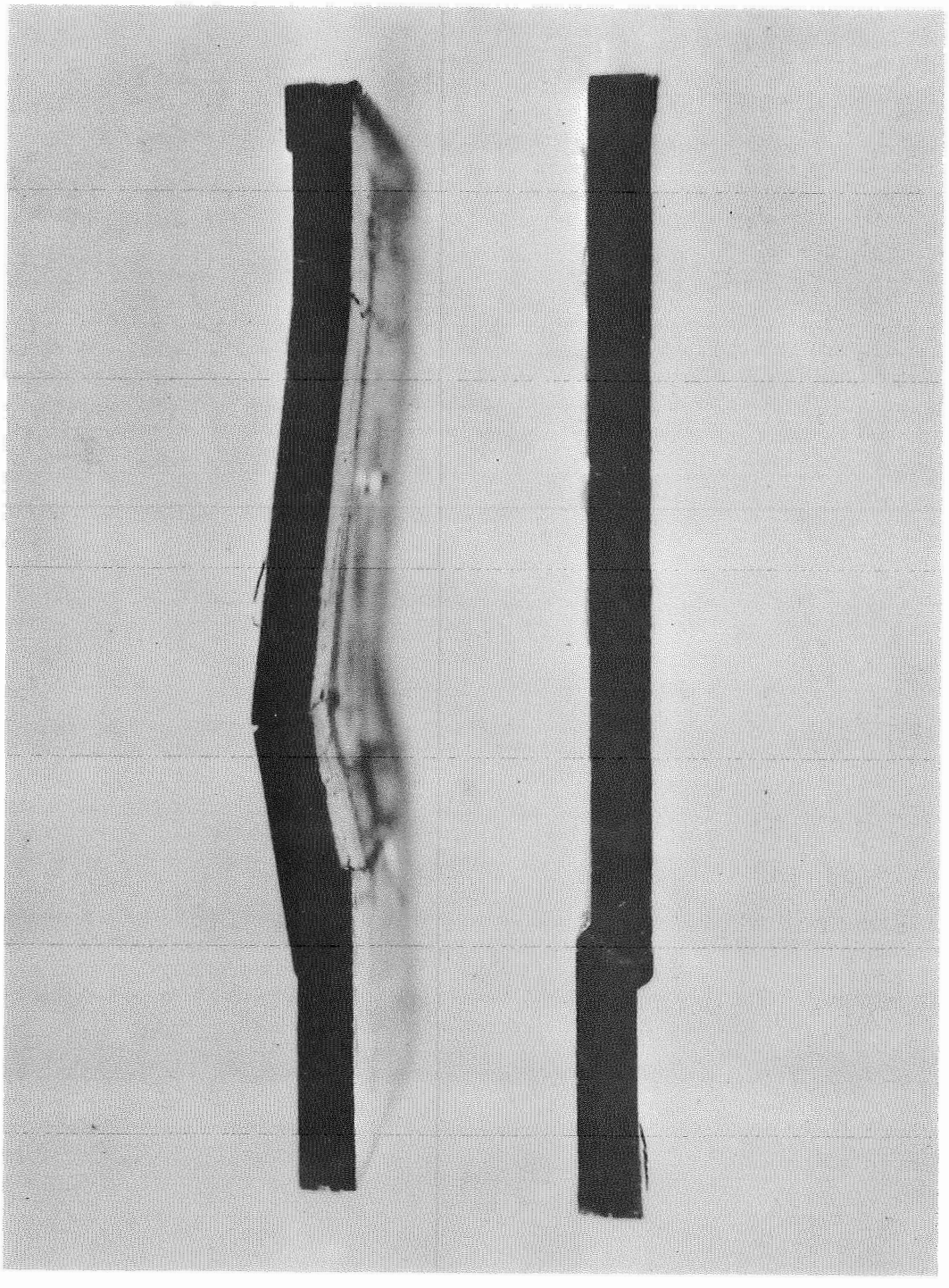

Figure 27

Modes of Compression Specimen Failure
Left - Gross Instability (Euler Buckling)
Right - Local Instability (Micro-Buckling)

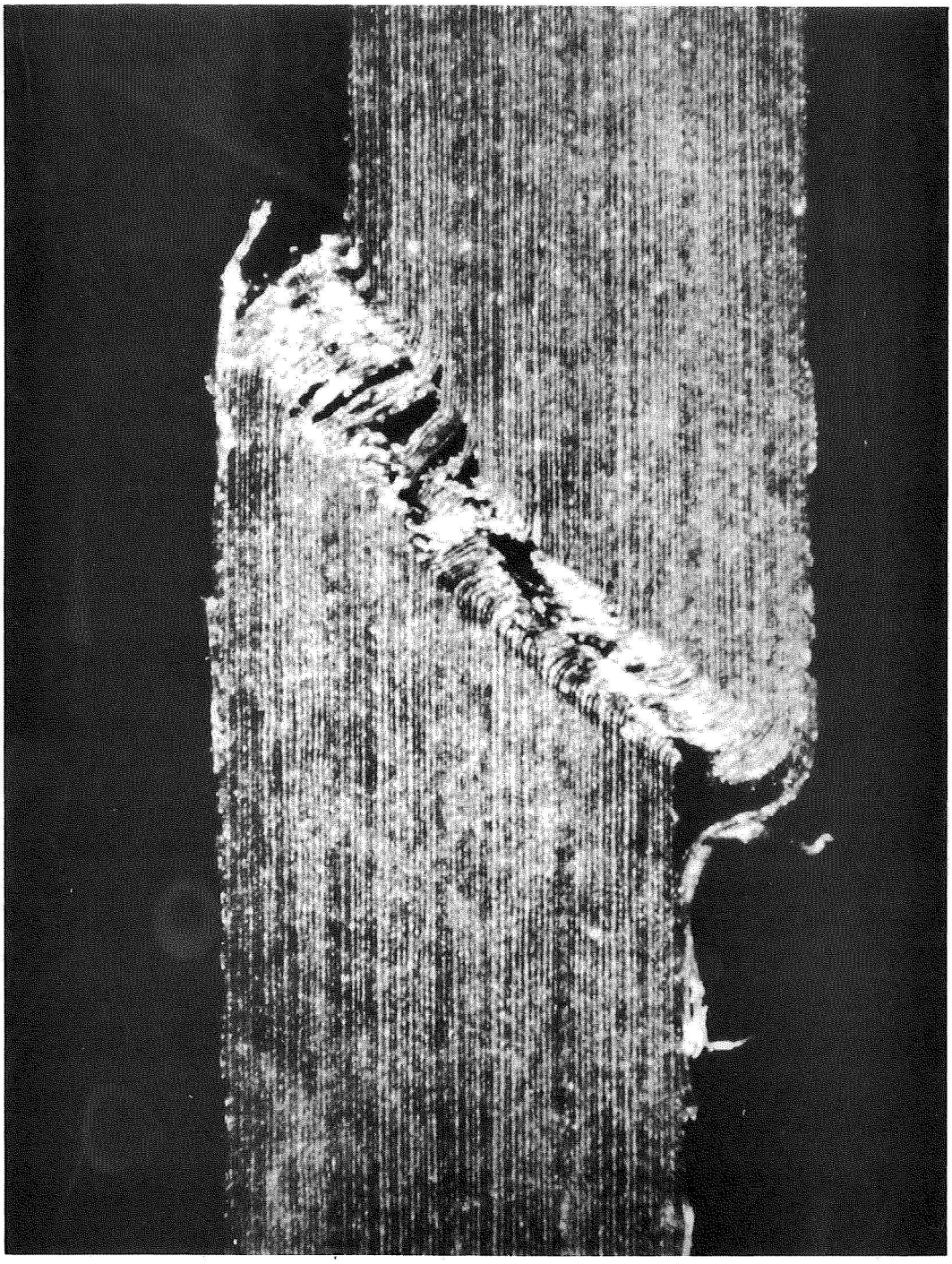

Figure 28

Detailed View of Boron Carbide
Laminate Compression Failure by Local Instability
(Specimen Edge Trimmed by Diamond Wheel Before Test,
Not Mounted Nor Polished After Failure, 20X)

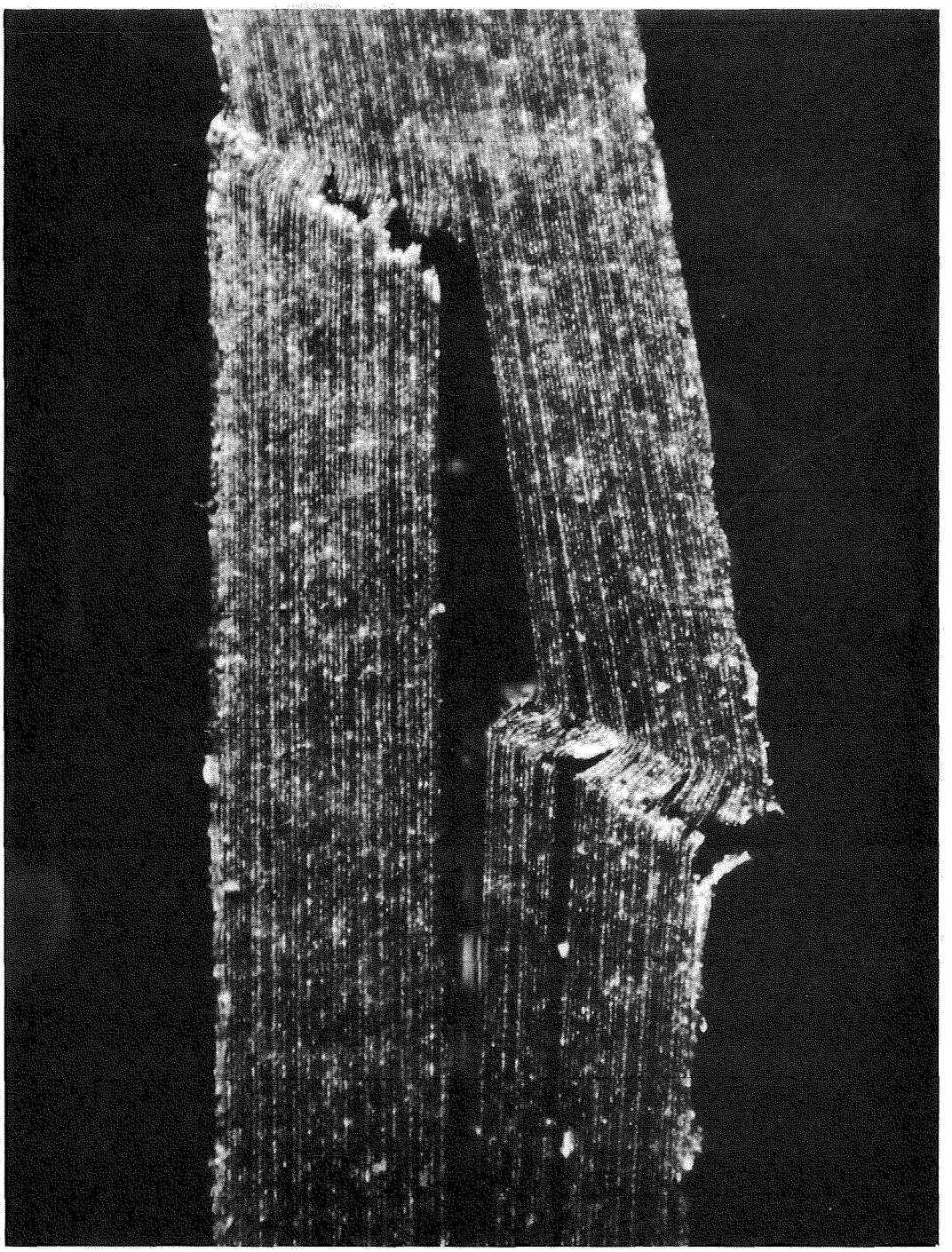

Figure 29

Detailed View of Boron Carbide Laminate
Compression Failure by Local Instability and
Interlaminar De-Cohesion
(Specimen Edge Trimmed by Diamond Wheel Before Test,
Not Mounted Nor Polished After Failure, 20X)

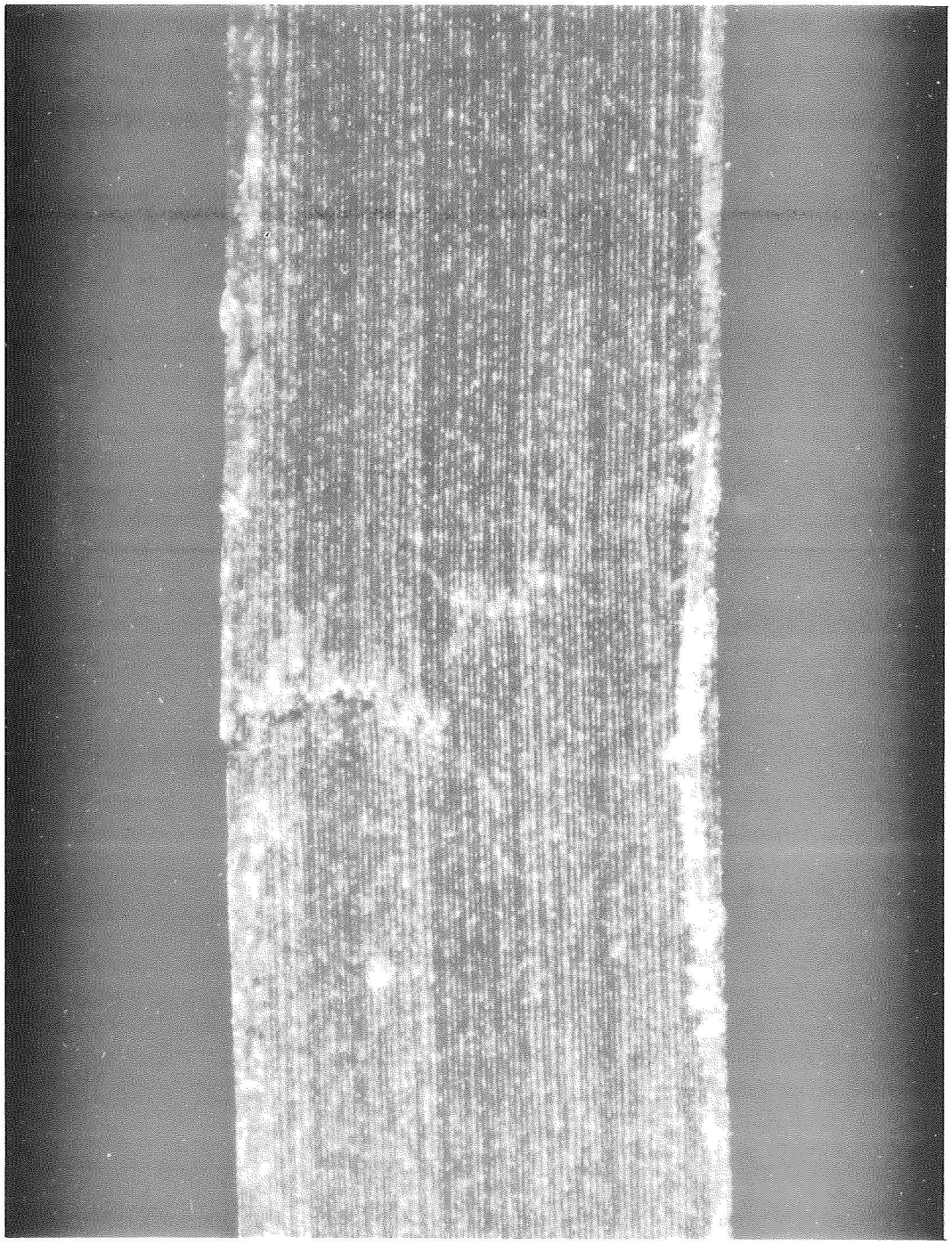

Figure 30

Mode of Failure of Boron Carbide
Interlaminar Shear Test Specimen
(Tension Failure Occurred Prior to Shear Failure, 20X)

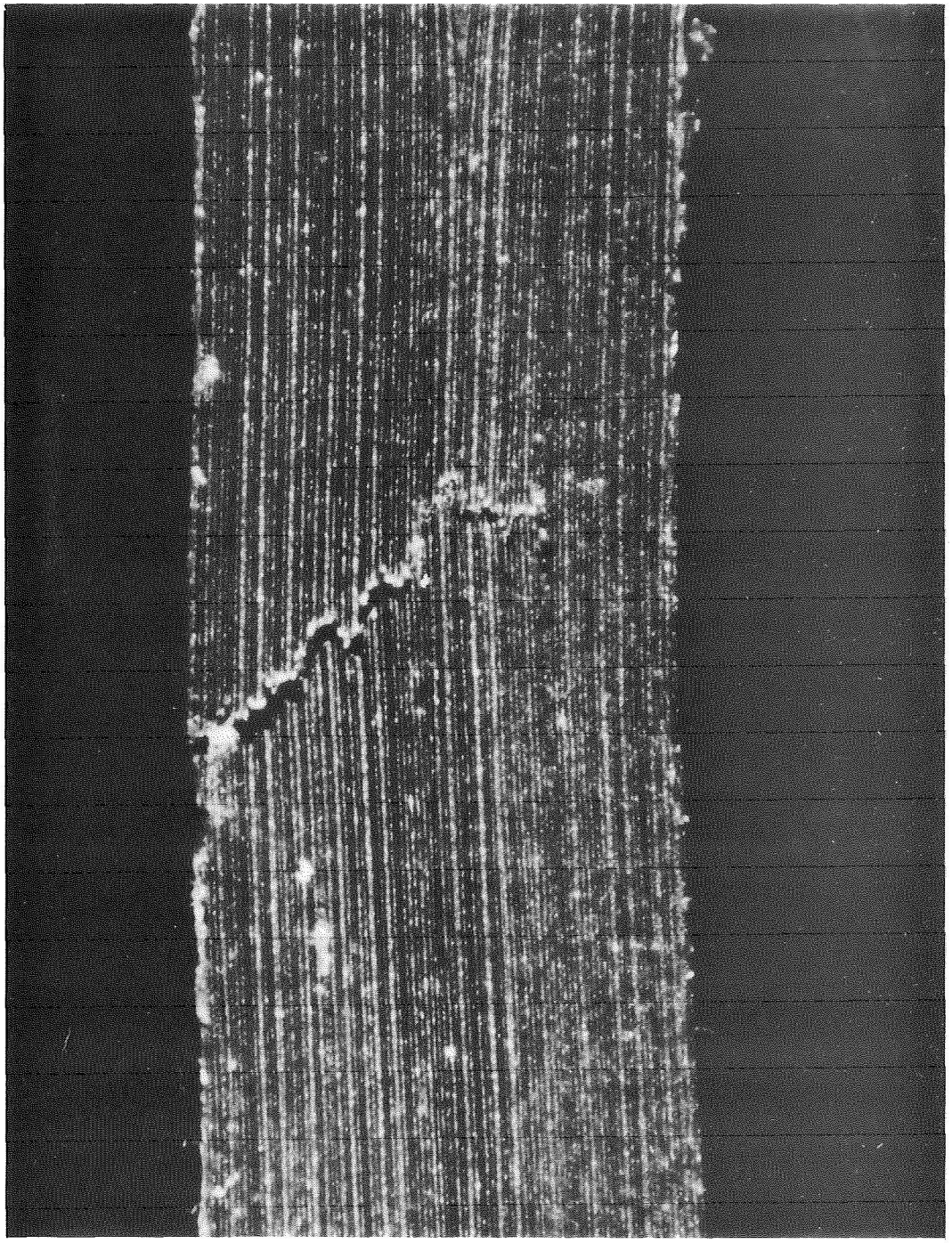

Figure 31

Mode of Failure of Boron Carbide
Interlaminar Shear Test Specimen
(Tension Failure Occurred Prior to Shear Failure, 20X)

solids, (i.e., highest symmetry) this relationship is

$$G = \frac{E}{2(1 + \mu)} \tag{9}$$

where E = Young's modulus of elasticity
μ = Poisson's ratio

Boron carbide sheet reinforced composites, though neither homogeneous nor isotropic in the strict sense of these terms, nevertheless behave as if they were when subject to plane stress loading. The torque/twist test, in particular, imposes a racking load which is primarily confined to the planes of the reinforcement layers. This component of the shear load is not transferred across the matrix/reinforcement interfaces except near the specimen edges and in the gripping areas. However, since the plate thickness was very small compared to the other specimen dimensions, the shear stress component in the direction of non-homogeneity (normal to the plane of the specimen) was a very small fraction of total shear load.

As a result, the elastic behavior of sheet reinforced composites subject to plane stress loads may be described by Eq. (9) with little error. This is in sharp contrast to the shear properties of fibrous composites which are strongly dependent on the fiber orientation and also diluted considerably by the weakening influence of the connecting matrix material. Poisson's ratio (μ) for boron carbide sheet reinforced composites has been measured as 0.1 to 0.2 (the variation may depend on specimen geometry and method of test). The validity of Eq. (9) when applied to the present set of specimens is illustrated in a plot of the shear

modulus (G) versus corresponding values of the bending modulus (E_F), Figure 32. A family of lines representing theoretical values of $G = G(E,\mu)$, computed for $\mu = 0$, 0.1, 0.2, 0.3, according to Eq. (9), has been superimposed on this plot for comparison. The results indicated a shear stiffness in both aluminum/epoxy and Kapton/epoxy matrix systems which apparently exceeded the expected value of G, even when the most favorable value of μ was assumed. This behavior may be characteristic for laminar quasi-isotropic composites in general, since the aluminum and the Kapton substrate systems were equally effective in developing such exceptional resistance to in-plane shear displacements.

Density and Specific Mechanical Properties

The density of the boron carbide reinforced laminates was rather uniform and very little dependent on the volume fraction of the reinforcement (inside the range of investigation). For aluminum substrate specimens, the density was 0.085 - 0.089 pci; for plastic resin substrate specimens, the range was 0.048 - 0.062 pci. Higher unit weight did not, in general, correspond with higher reinforcement content, but seemed to be influenced more by the adhesive layer thickness.

The specific modulus (E_F/ρ) ranged from 1.43 up to 2.63×10^8 in. The upper value compared favorably with about 1×10^8 in. for aluminum and titanium, and also with 2.60×10^8 in. for (0°, 90°) biaxial boron filament reinforced resin composites containing the maximum fiber loading of 62 volume percent. It is important to note, however, that E/ρ for film reinforced composites remains virtually constant in any orientation, whereas the value of 2.60×10^8 in. for the biaxial fibrous composite is developed only parallel/transverse

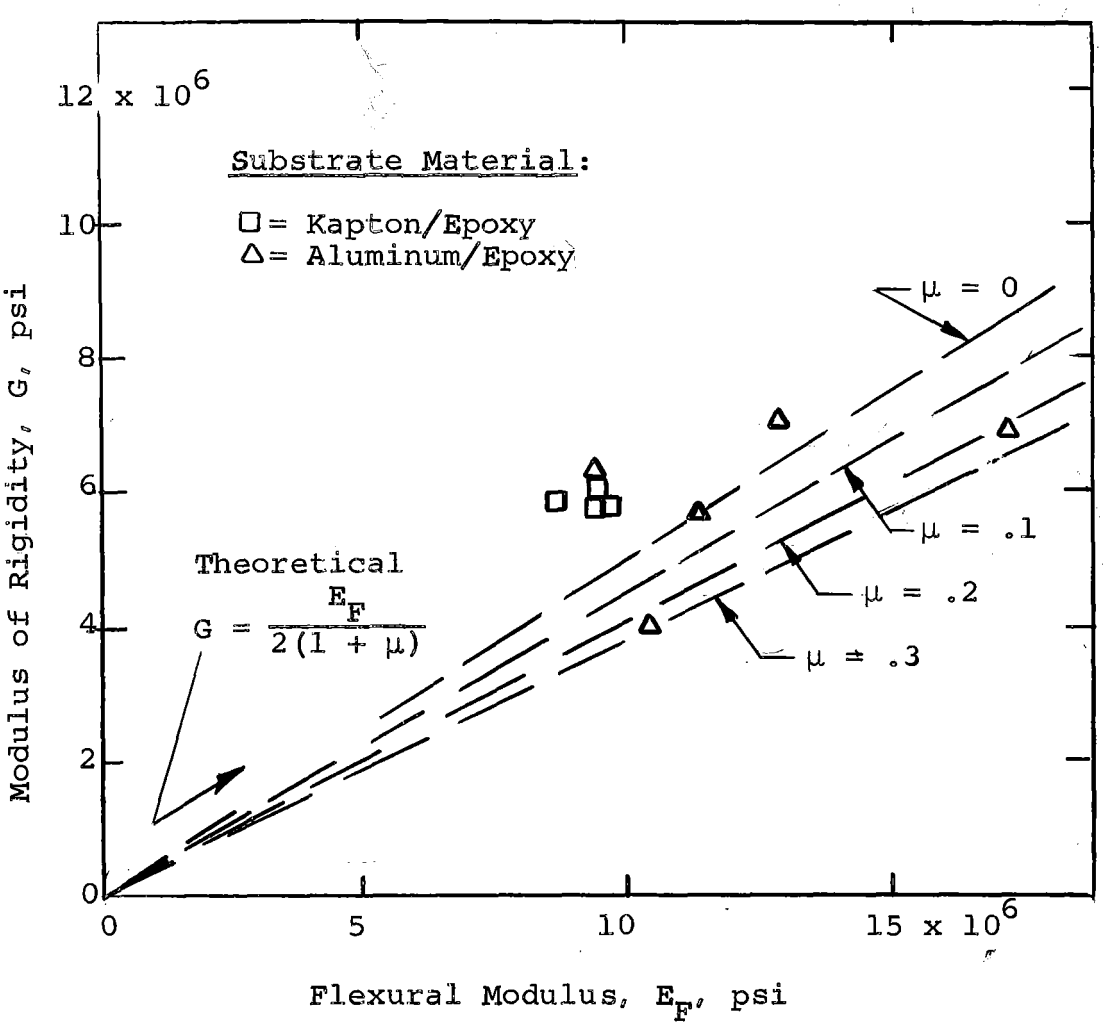

Figure 32

The Measured Modulus of Rigidity, G, Compared to Values Predicted by Elastic Theory

to the fibers. At ±45°, the specific bending modulus is down to 0.4 x 10^8 in.[10]

The specific strength (σ/ρ) ranged from about 2 to 5 x 10^5 in., with the best value of 5.16 x 10^5 in. achieved in the boron carbide/Kapton system. These values are not very good, being exceeded by some aircraft metals (8 to 10 x 10^5 in.) and by filamentary composites (from 1 and up to 30 x 10^5 in., depending on fiber orientation and volume fraction).

Summary of Results

The salient results of the mechanical testing may be summarized as follows:

(1) The laminates developed good stiffness in the elastic range, with an observed range of 60 to 100 percent effectiveness of the reinforcement, based on the volume percent present. This stiffness was virtually independent of orientation in the plane of the specimen plates.

(2) The tensile strength of the composites was limited by two factors. First, the intrinsic strength of the reinforcement apparently did not exceed 160,000 psi at best; and second, the highest volume fraction of reinforcement was not greater than about 30 percent.

(3) It appeared that Kapton was a much better substrate for boron carbide reinforcement deposition than aluminum foil. The cause has not been determined.

(4) Sheet reinforced laminar composites exhibited an unusually high degree of shear stiffness when subjected to in-plane shear loading, exceeding by more than 40 percent the value predicted for an isotropic material.

(5) No explanation was available for the discrepancy between the higher strength capabilities of boron carbide

film deduced from the taper bar test, and the lower strength behavior observed in the fabricated composite specimens.

(6) Specific flexure moduli up to 2.63×10^8 in. and specific tensile strengths up to 5.16×10^5 in. have been observed.

8. Conclusions

The main conclusions drawn from the present program are:

(1) Boron carbide may be evaporated in vacuum using electron beam techniques. The vapor may be condensed on both aluminum foil and polyimide films to produce thin adherent coats.

(2) The chemical composition of the deposits tended to be slightly carbon-rich, compared to the source material, which in turn contained a small excess of carbon compared to stiochiometric boron carbide. It has not been determined if the film strength depends on its exact chemical composition. The film stiffness was close to the value of 60×10^6 psi reported in the literature, independent of composition.

(3) The tensile fracture strength of boron carbide films deposited on massive substrates was computed to be on the order of 300,000 psi.

(4) The surface morphology of the boron carbide films as deduced from optical and electron micrography showed low degrees of physical imperfections in many instances. The major type of flaw appeared to result from the deposition of globular particles on the order of 1×10^{-4} inch in diameter which were superficial on, or partially embedded in, the surface. These non-homogeneities and flaws may be the major causes for reduced strength in the films deposited on thin polyimide and aluminum substrates.

(5) X-ray diffraction studies indicated that the films are "amorphous" in character with estimated crystallite sizes of less than 50Å. High crystallinity therefore is not expected to be a strength limiting factor.

(6) Procedures have been developed for the fabrication of multilayer laminates of boron carbide on both aluminum and

polyimide substrates using Union Carbide epoxy adhesive ERL-2256. This adhesive appears superior to the phenoxy adhesive used early in the program.

(7) The mechanical properties of boron carbide reinforced laminar composites included high elastic bending and shear stiffness and moderate strength. These properties were virtually independent of orientation.

(8) The highest strength developed in the reinforcement phase was about 160,000 psi as calculated by the Rule-of-Mixtures. This was substantially lower than the potential fracture strength of 300,000 psi or better which was exhibited by the film when deposited on thick substrates. The cause of this descrepancy was not determined in this investigation.

9. Recommendations

The results of this program indicate that boron carbide laminate composites have high potential for applications where minimum weight structural materials are required. In order to develop the potential of these composites it is recommended that future work be directed to the following:

(1) Improved laminate strength. Further work is required to identify the surface flaws and defects which may be strength controlling. Morphology studies should be used to improve deformation and handling techniques so as to reduce or eliminate flaws.

(2) Efforts should be made to increase the volume fraction of reinforcement in the composite. The use of presently available substrates which are thinner than those used in the present contract appears promising. Increased moduli and strengths should result.

(3) Methods need to be developed to improve the degree of adhesion of boron carbide to plastic substrates, such as the polyimide film.

(4) More fundamental work is required to relate the effects of deposition parameters--rate of evaporation, temperature of substrate, etc.--to the basic properties of the film--density, composition, strength, etc. Fundamental work is required on the inhomogeneous residual stresses which may develop between the substrate and film, and within the deposit itself.

10. Acknowledgment

The authors wish to thank Professor A. S. Argon, Mechanical Engineering Department, Massachusetts Institute of Technology, for his assistance and suggestions -- particularly with respect to the strength measurements of the film deposits.

REFERENCES

1. Chadsey, E. E., and L. R. Allen, Technical Report AFML-TR-66-354, October 1966, Air Force Materials Laboratory, Wright-Patterson Air Force Base, Ohio 45433.

2. Beecher, N., F. Feakes and L. R. Allen, 12th Material SAMPE Symposium, Vol. 12, NR3, Anaheim, California, October 10-12, 1967.

3. Chadsey, E. E., and F. Feakes, Summary Report, Contract No. F33615-67-C-1447, Air Force Materials Laboratory, March 7, 1967.

4. Verhaegen, G., J. Chem. Phys., 37, 13367, (1962).

5. Verhaegen, G., et al, Nature 193, 1280, (1962).

6. Elliott, R. P., IIT Research Institute, ARF-2200-12, Final Report on U. S. Atomic Energy Commission Contract At(11-1)-578, Project Agreement No. 4, June 1961.

7. G. V. Samsonore, N. Zhuravlev and I. G. Amnuel, Fiz. Metal, Metalloved 3, 309-313, (1956).

8. Stephen W. Tsai, "Experimental Determination of the Elastic Behavior of Orthotropic Plates". Jour. of Engineering for Industry, Aug. 1965, p. 315.

9. R. L. Foye, "Deflection Limits on the Plate-Twisting Test". Jour. Composite Materials, Vol. 1, p. 194, (1967).

10. V. Grinius, Micromechanics - Experimental and Analytical Studies, AFML-TR-67-148, (October 1967).

APPENDIX I

DERIVATION OF THE CRACK FORMATION LIMIT

DERIVATION OF THE CRACK FORMATION LIMIT

$$f \cdot \epsilon = \text{constant.}$$

The description of the post-critical strain region $\epsilon > \epsilon_{cr}$ by means of the linear coefficient, **A** , was based on the following consideration.

The shear traction, τ , needed to fracture again a segment of the cracked boron carbide film is determined by static equilibrium, and must be no less than

$$\tau > \frac{2\sigma t}{\ell} \qquad \text{(A1)}$$

assuming, in the limit, purely plastic behavior of the titanium substrate; σ is the fracture strength, t is the thickness, and ℓ is the current length of the film segment under consideration. We can also assume perfect elasticity in the brittle coating with littler error, so

$$\sigma = \epsilon E \qquad \text{(A2)}$$

where ϵ is the elastic strain, and **E** is the elastic modulus of the boron carbide. Furthermore,

$$\frac{1}{\ell} = f \qquad \text{(A3)}$$

by the definition of **f** . Combining (A1), (A2), and (A3) we get

$$f \cdot \epsilon < \frac{\tau}{2Et} \qquad \text{(A4)}$$

The right hand side of (A4) can be evaluated approximately since $t = 0.35 \times 10^{-3}$ in., $E = 6 \times 10^{7}$ psi, and $\tau = 1/2\ \sigma_y$. (σ_y is the tensile yield stress $\approx 50 \times 10^{3}$ psi for commercially pure titanium). Then, approximately,

$$f \cdot \epsilon < 0.6\ (\text{in.}^{-1}) \qquad \text{(A5)}$$

Thus, 0.6 (in.^{-1}) is an upper bound for the product $(f \cdot \epsilon)$, and the density of cracks cannot increase further, consistent with the assumption of purely plastic behavior $\tau < \sigma_y/2$. If this assumption is relaxed and strain hardening in the titanium is accounted for, then $f \cdot \epsilon$ could increase further, but at a slower rate.

The theoretical curve $f \cdot \epsilon = \text{constant} = 0.6\ (\text{in.}^{-1})$ has been drawn in Figure 3. It is in good agreement with the observed behavior, since an unmistakable decrease in the observed crack formation rates $\frac{df}{d\epsilon}$ occurred beyond this theoretical curve. The "bending over" of the crack density vs. strain curves beyond this limit, therefore, reflects chiefly the plastic strain hardening behavior of the titanium substrate. The f vs. ϵ curves below this line, however, do represent the strain-sensitivity of crack formation in the boron carbide coated films. In this region, the linear relationship as expressed by the coefficient (A) is a good approximation.